JOURNAL OF GEOPHYSICAL RESEARCH, VOL. 112, A02202, doi:10.1029/2006JA011877, 2007

Correction published 2 June 2007

Separator reconnection at Earth's dayside magnetopause under generic northward interplanetary magnetic field conditions

John C. Dorelli,[1] Amitava Bhattacharjee,[1] and Joachim Raeder[1]

Received 2 June 2006; revised 18 August 2006; accepted 13 October 2006; published 14 February 2007.

[1] We investigate the global properties of magnetic reconnection at the dayside terrestrial magnetopause under generic northward interplanetary magnetic field (IMF) conditions. In particular, we consider a zero dipole tilt case where the y and z components of the IMF (in GSM coordinates) are equal in magnitude, using three-dimensional resistive magnetohydrodynamics (MHD) simulations to address the following questions: (1) What is the geometry of the dayside X line? (2) How is current density distributed over the magnetopause surface? Using a technique described by Greene* (1992) to track the magnetic nulls in the system, we identify the dayside X line as a magnetic separator line, a segment of a magnetic field line which extends across the dayside magnetopause, terminating in the cusps. We demonstrate that the separator line is the intersection of two separatrix surfaces which define volumes containing topologically distinct field lines. Parallel current density, proportional to the parallel electric field in our resistive MHD simulations, is distributed in a broad, thin sheet which extends across the separator line and terminates in the cusps. Thus separator reconnection at the dayside magnetopause displays features of both antiparallel (near the cusp nulls) and component (near the subsolar separator line) reconnection. We discuss some implications of our results for spacecraft observations of reconnection signatures.

Citation: Dorelli, J. C., A. Bhattacharjee, and J. Raeder (2007), Separator reconnection at Earth's dayside magnetopause under generic northward interplanetary magnetic field conditions, *J. Geophys. Res.*, *112*, A02202, doi:10.1029/2006JA011877.

1. Introduction

[2] The global topology of the dayside magnetopause remains something of a puzzle, despite the observational evidence in favor of *Dungey*'s [1961, 1963] reconnecting magnetosphere model which has accumulated over the last several decades. When the interplanetary magnetic field (IMF) is due northward (in this paper we shall focus exclusively on northward IMF conditions), we are accustomed to visualizing magnetospheric reconnection by projecting the magnetic field onto the noon-midnight meridional plane, as illustrated in Figure 1. In such a projection, one naturally identifies the magnetic neutral points (contained within the yellow regions in Figure 1) as potential sites of magnetic reconnection. If the magnetosphere were two-dimensional, such neutral points would correspond to the projections of neutral lines extending infinitely in both directions normal to the noon-midnight meridional plane. Such neutral lines would define the locations where magnetic separatrices (solid black lines) intersect to define the usual three topologically distinct sets of magnetic field lines: (1) solar wind field lines, which extend to infinity in both directions (red lines); (2) open field lines, which extend to infinity in one direction and intersect Earth's ionosphere in the other (green lines); and (3) closed field lines, which intersect Earth's ionosphere in both directions (blue lines). It is well known that such neutral lines have a tendency to collapse into thin current sheets [*Dungey*, 1953; *Parker*, 1957; *Imshennik and Syrovatsky*, 1967; *Syrovatsky*, 1971] (Figure 2) within which the non-MHD terms in the generalized Ohm's law (e.g., Hall electric fields, electron pressure tensor, electron inertia, etc.) become important.

[3] In the two-dimensional context of Figure 1, there are two null lines (N_1 and N_2), each of which is defined by the intersection of two separatrix surfaces which extend infinitely out of the plane of the figure. Thus it is natural to view the formation of thin current sheets at the null lines as two independent X line collapse processes. When Earth's dipole axis is antiparallel to the IMF, a particular solar wind field line convecting through the magnetosheath will make contact with N_1 and N_2 simultaneously. In a two-dimensional magnetosphere (or in three dimensions if the two null lines are long enough), such simultaneous contact of a solar wind field line with northern and southern lobe field lines would still occur in the presence of a magnetic field component out of the plane; a dipole tilt (such that Earth's dipole axis is not parallel to the IMF) would be required to preclude such simultaneous contact (e.g., see *Crooker* [1992] for a discussion of the effects of dipole tilt on magnetospheric magnetic field topology and ionospheric convection patterns).

[1]EOS Space Science Center, University of New Hampshire, Durham, New Hampshire, USA.

0148-0227/07/2006JA011877$09.00

*The name is correct here. The article as originally published is online.

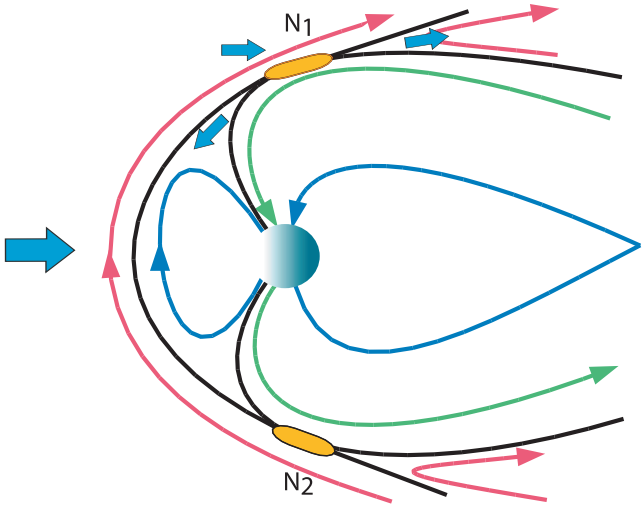

Figure 1. This figure illustrates reconnection in a two-dimensional magnetosphere under northward IMF conditions. The Sun is to the left. Thick blue arrows show plasma bulk velocity vectors. Closed magnetic field lines (with both ends connected to Earth) are shown in blue; open field lines (with one end connected to Earth) are shown in green; solar wind field lines (with neither end connected to Earth) are shown in red. Diffusion regions surrounding X type null lines (marked "N_1" and "N_2") are shown as orange ovals, while the black lines show the corresponding separatrix surfaces.

[4] Figure 3 (adapted from *Cowley* [1983]) illustrates the effect of dipole tilt on the magnetic field topology of Figure 1. Again, one views reconnection as a local process, with two separate current sheets associated with the two distinct null lines. However, owing to the dipole tilt, there is no longer a field line joining the two null lines. If one follows a particular solar wind field line as it convects through the magnetosheath, it will make first contact with a lobe field line at N_1, producing a new open field line. Later, the new open field line will make contact with the southern cusp null, N_2, producing a new closed field line on the dayside.

1.1. Defining Three-Dimensional Magnetic Reconnection

[5] *Vasyliunas* [1975] defines magnetic reconnection as the process by which plasma flows across surfaces which separate volumes containing topologically distinct classes of magnetic field lines. In two dimensions, this definition is robust, since two-dimensional X lines are structurally stable; that is, such null lines survive generic (nonideal) two-dimensional perturbations of the magnetic field. Nevertheless, as *Schindler and Hesse* [1988] and *Hesse and Schindler* [1988] point out, extending this definition to three dimensional magnetic fields is problematic since magnetic neutral lines (and associated separatrix surfaces) do not survive generic perturbations of the magnetic field in three dimensions (see *Greene* [1988] and *Lau and Finn* [1990] for further discussion of the structural instability of two-dimensional neutral lines). Thus *Schindler and Hesse* [1988] and *Hesse and Schindler* [1988] advocate a more general definition based on an earlier formulation by *Axford* [1984]: magnetic reconnection occurs whenever a spatially localized parallel electric field causes the magnetic field to evolve in time in such a way that two plasma fluid elements initially threaded by a field line are, at a later time, no longer threaded by the same field line.

[6] Both of the above definitions suffer from a degree of arbitrariness, relying on a particular identification of "plasma flows." For example, in resistive MHD, "plasma flow" refers to the center of mass bulk velocity. Nevertheless, even in a plasma with a nonvanishing parallel electric field, one can often find another field line velocity which preserves the magnetic field topology. Indeed, one can, in general, find many field line velocities to describe the same magnetic field evolution [*Newcomb*, 1958; *Vasyliunas*, 1972]. The essential point is that one cannot infer, from the fact that the center of mass bulk velocity is not a field line velocity, that the magnetic field topology is changing or that magnetic flux within topologically distinct flux domains is changing. For example, in the context of resistive Hall MHD, the electron bulk velocity is a field line velocity in the limit of zero resistivity.

[7] *Boozer* [2002] defines magnetic reconnection as spatially localized nonideal magnetic field evolution. Here, "ideal magnetic field evolution" refers to evolution which satisfies the following equation:

$$\frac{\partial \mathbf{B}}{\partial t} + \mathbf{V_B} \cdot \nabla \mathbf{B} = \mathbf{B} \cdot \nabla \mathbf{V_B} - \mathbf{B}(\nabla \cdot \mathbf{V_B}) \tag{1}$$

where $\mathbf{B}$ is the magnetic field and $\mathbf{V_B}$ is a continuous velocity field (not necessarily differentiable or even associated with fluid motion). Equation (1), which implies that the magnetic flux in any given flux tube is preserved, is consistent with Faraday's law if and only if the electric field, $\mathbf{E}$, can be written as follows:

$$\mathbf{E} = -\mathbf{V_B} \times \mathbf{B} + \mathbf{R} \tag{2}$$

such that $\nabla \times \mathbf{R} = 0$. Note that *Boozer* [2002] distinguishes "ideal magnetic field evolution" (magnetic flux conservation) from "ideal MHD." That is, equation (1) is consistent with a nonvanishing parallel electric field so long as $\mathbf{R} = -\nabla\Phi$, where Φ is a smooth scalar function which satisfies the magnetic differential equation:

$$\mathbf{B} \cdot \nabla\Phi = E_{\|}. \tag{3}$$

For example, if the line integral of the electric field around a closed field line is nonvanishing, then one cannot find a single valued Φ satisfying (3); hence the magnetic flux threading the closed field line is not conserved and reconnection occurs (e.g., magnetic island formation on a resonant surface in a toroidal magnetic field configuration is an example of such reconnection). On the other hand, if the magnetic field is time stationary, then the line integral of the electric field around any closed path in the system vanishes, so the necessary condition (3) for ideal magnetic field evolution is satisfied (note that boundary conditions may still preclude the existence of a smooth Φ); further, the trivial zero field line velocity implies flux conservation, despite the fact that the plasma is nonideal.

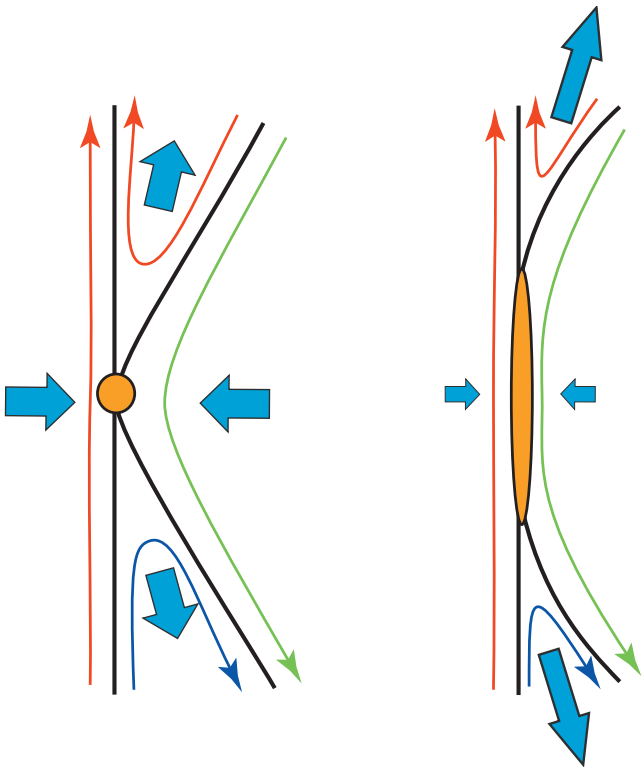

Figure 2. This cartoon illustrates X line collapse. The left figure shows an X type neutral line with low current density. The low current configuration is unstable to a small perturbation in the component of the current density into the page. Such a perturbation induces a plasma flow (thick blue arrows) which acts to reinforce the current perturbation, resulting in a collapse of the X line into a thin current sheet with a double Y separatrix geometry (see *Priest and Forbes* [2000] for a review of the theory of X line collapse).

[8] While the *Boozer* [2002] definition of reconnection removes the arbitrariness of the *Vasyliunas* [1968] and *Schindler and Hesse* [1988] definitions (since it makes no reference to plasma bulk velocities), it is too restrictive for our purpose, since it excludes steady reconnection in a finite system with nonvanishing Poynting flux on the boundaries. For example, in the magnetosphere, reconnection is steady if the line integral of the parallel electric field around the separator vanishes, so that the polar cap flux does not change in time. Nevertheless, in steady state, the line integral of $E_{||}$ along any closed magnetic field line vanishes, so one can solve (3) for a smooth Φ (given appropriate boundary conditions). Indeed, in steady state, the field lines can be viewed as moving with zero velocity. Thus to accommodate steady reconnection, we adopt a weaker definition. Magnetic reconnection occurs whenever the following two conditions are satisfied: (1) the magnetic field can be divided into topologically distinct flux volumes which are defined by intersecting separatrix surfaces; (2) the parallel electric field is nonvanishing at one or more locations on the intersections of the separatrix surfaces. While this definition excludes cases which have traditionally been viewed as reconnection, but for which separatrix surfaces do not exist (the *Schindler and Hesse* [1988] example of a finite-length plasmoid in the magnetotail is a good example), we think that the definition represents the most straightforward generalization of the intuitive idea of magnetic reconnection proposed by *Vasyliunas* [1975].

[9] *Lau and Finn* [1990] review the kinematics of three-dimensional magnetic reconnection, working out the effects, in the ideal MHD limit, of singular magnetic field structures (nulls, separator lines, and separatrix surfaces) on the mapping of the electric potential along magnetic field lines. The simplest such singular magnetic field structure is an isolated magnetic null. If the magnetic field, **B**, is sufficiently well behaved near the null, one can Taylor expand around the null as follows: $\mathbf{B}(\mathbf{r}) \approx \mathbf{r} \cdot \nabla \mathbf{B}$. One then classifies magnetic nulls according to the eigenvalues of the $\nabla \mathbf{B}$ matrix (denote them by λ, μ, ν). Since the magnetic field has vanishing divergence, the trace of $\nabla \mathbf{B}$ vanishes: $\lambda + \nu + \mu = 0$. As discussed by *Lau and Finn* [1990] (we will follow their terminology, originally introduced by *Cowley* [1973], in this paper), there are several cases to consider: (1) one of the eigenvalues vanishes, and the other two are either real (corresponding to a two-dimensional X line) or complex conjugate (corresponding to an O line); (2) all three eigenvalues are real, and one is positive (type A null) or one is negative (type B null); (3) one of the eigenvalues is real and the other two are complex conjugates (if the real eigenvalue is positive, the null is a type A_S null; if the real eigenvalue is negative, the null is a type B_S null).

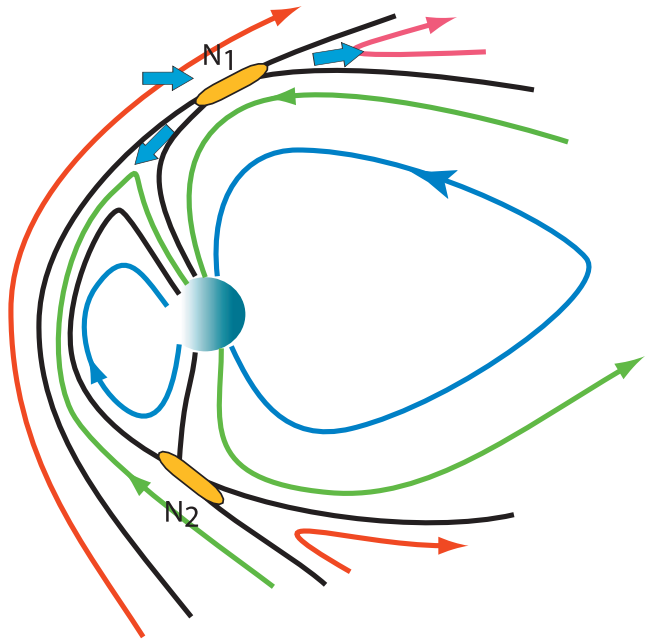

Figure 3. This figure illustrates the effect of tilting Earth's dipole axis in two dimensions. As in Figure 1, solar wind field lines (with neither end connected to Earth) are shown in red, open field lines (with one end connected to Earth) are shown in green, and close field lines (with both ends connected to Earth) are shown in blue. The separatrix surfaces are drawn in black. Note that there is no longer a single field line which passes through both N_1 and N_2. A solar wind field line convecting through the magnetosheath will encounter N_1 earlier than N_2.

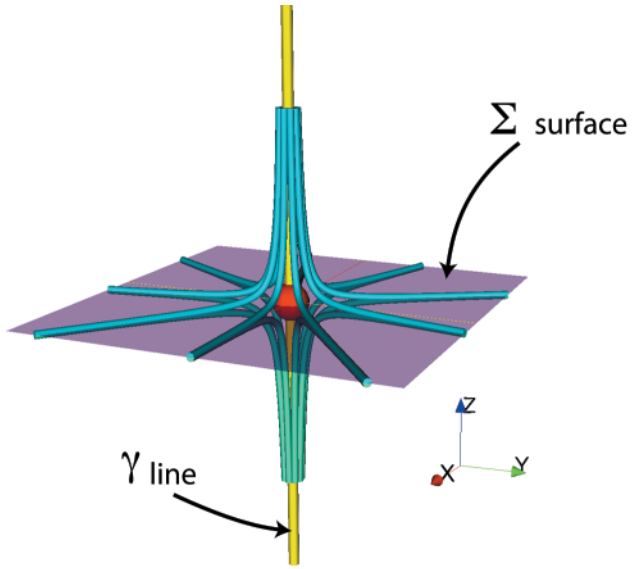

Figure 4. This figure illustrates the magnetic field topology local to an isolated magnetic null. The null is the red sphere. The γ (spine) curve is shown in yellow; the Σ (fan) surface, which is a separatrix defining two topologically distinct flux domains, is the translucent purple plane.

[10] For example, Figure 4 shows the case where $B_x = x$, $B_y = y$, and $B_z = -2z$. This is a type B null, since the three ∇ **B** eigenvalues are real and there is one negative eigenvalue: $\lambda = 1$, $\mu = 1$, and $\nu = -2$. The yellow line (the γ line), corresponding to the negative eigenvalue, is a field line such that the magnetic field always points toward the null. The purple plane (the Σ surface) corresponds to the two positive eigenvalues: the field lines in this plane all point away from the null. For an isolated type A null, all of the field directions are reversed. Note that there is an important qualitative difference between two-dimensional nulls and three-dimensional nulls. In the two-dimensional case there are two separatrix curves which define domains containing different topological classes of field lines (as illustrated, for example, in Figure 2). However, in the three-dimensional case, there is only one separatrix surface: the Σ surface. Thus reconnection associated with an isolated three-dimensional null is qualitatively different from reconnection at a two-dimensional null (see *Priest and Forbes* [2000] for a discussion of the different types of reconnection which can occur at an isolated three-dimensional null).

[11] In a system with two magnetic nulls of opposite types (as shown in Figures 5 and 6), the Σ surfaces associated with the two nulls intersect, in general, to form a separator line, a single magnetic field line which joins the two nulls. If one projects the magnetic field onto any plane perpendicular to the separator line, then the projected field has an X type null at the point where the separator crosses the plane; and the two associated separatrices correspond to the intersections of the Σ surfaces with the plane. Thus one can view the separator as the three-dimensional analogue of the standard two-dimensional X line topology, with a guide field that varies along the X line. However, note that in three dimensions we require two nulls (a type A and a type B) to produce such an X line topology; in two-dimensions, such a topology (with two separatrix surfaces) occurs near a single null.

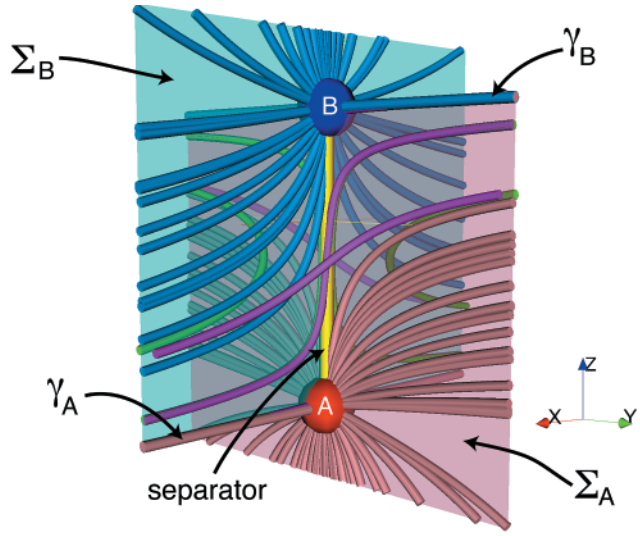

Figure 5. This figure illustrates the topology of separator reconnection. In this configuration there are two magnetic nulls: a type A null (red sphere) and a type B null (blue sphere). The two nulls are joined by the yellow field line, which points from the B null to the A null. This singular field line is the separator line, the three-dimensional analogue of the two-dimensional X line; it is defined by the intersection of the two Σ surfaces, which play roles analogous to those played by two-dimensional separatrices associated with a single X type null).

1.2. Three-Dimensional Reconnection at Earth's Dayside Magnetopause

[12] In three dimensions the magnetic field topology under exactly northward IMF conditions differs qualitatively

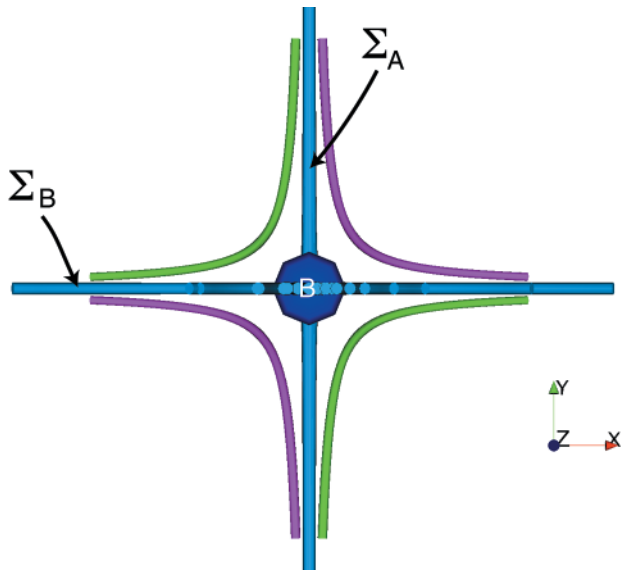

Figure 6. This figure shows a bird's eye view (looking down at the origin from a point along the positive z axis) of the separator topology shown in Figure 5.

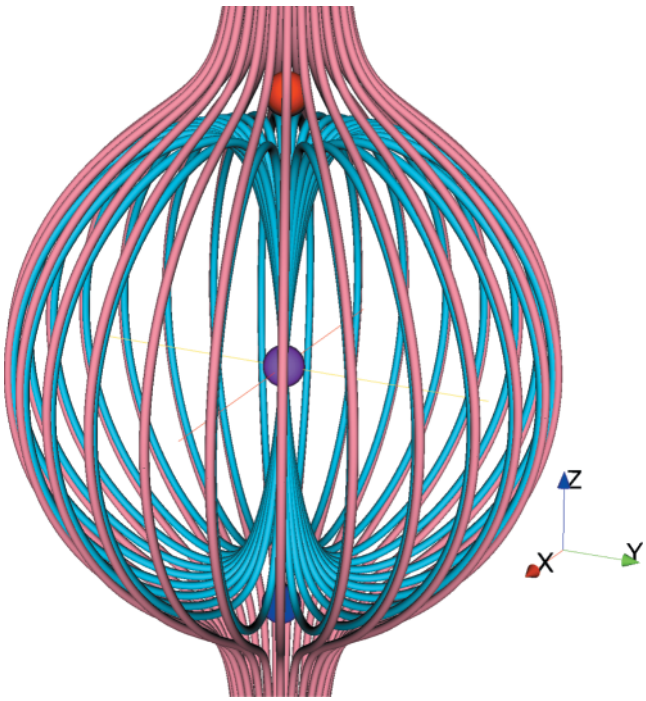

Figure 7. This figure shows a three-dimensional view of the vacuum superposition topology which forms the basis of Dungey's pure northward IMF reconnecting magnetosphere model. Solar wind field lines (light red) are separated from closed magnetospheric field lines (light blue) by a spherical separatrix surface. The red and blue spheres show the locations of the two cusp nulls, one in each hemisphere, at which the magnetic field vanishes.

from that shown in Figure 1. Figure 7 shows the magnetic field topology of a vacuum superposition (in which a uniform IMF is superimposed on a dipole field) for the case where the dipole tilt is zero and the IMF is due northward. Unlike the situation in Figure 1, in which there are two distinct separatrix surfaces which intersect to form two distinct null lines, in Figure 7 there is only a single surface which separates solar wind field lines from closed magnetospheric field lines. The separatrix consists of an infinite number of field lines which join the two cusp nulls (shown as red and blue spheres in the Figure 7) (a topologically equivalent plasma equilibrium, with non-vanishing current density on the spherical surface, was considered by *Hu et al.* [2004] in their study of the linear spherical tearing mode).

[13] The spherical separatrix surface of Figure 7 is structurally unstable; that is, the surface does not survive general (nonideal) perturbations of the magnetic field. For example, *Russell* [1972] points out that when the IMF clock angle is nonzero, a particular solar wind field line will generally encounter an antiparallel (or nearly antiparallel) lobe magnetic field only in a single hemisphere. Figure 8 illustrates the idea in the context of the vacuum superposition topology (the IMF clock angle is 45 degrees in the figure, but the topology is the same for all IMF orientations). Solar wind field lines which make contact with tail lobe field lines in one hemisphere (in this context, at one of the two cusp nulls, the red and blue spheres in Figure 8) transform into newly opened field lines (shown in green) which drape over the magnetosphere in opposite senses on the dawnside and duskside (the Sun is in the positive X direction in the figure).

[14] In the vacuum superposition topology, there is a single field line (shown in yellow in Figure 8) joining the two cusp nulls. While one can identify this field line as a solar wind field line (shown in red) which makes simultaneous contact with the two cusp nulls, one cannot, by inspection of the magnetic field topology alone, identify magnetic reconnection as a local process occurring at the nulls (as one does in two dimensions). Figure 9 shows the magnetic skeleton of a generic vacuum superposition, visualized by computing magnetic field streamlines corresponding to seed points distributed randomly within small spheres surrounding each magnetic null (100 seed points per null). Each such set of field lines maps out a separatrix surface, one for each null. Red field lines correspond to the northern null (depicted by a red sphere); blue field lines correspond to the southern null (depicted by the blue sphere). Thus in the generic case, in which the dipole and IMF axes are not aligned, the single separatrix surface of Figure 7 bifurcates into two distinct surfaces. The closed

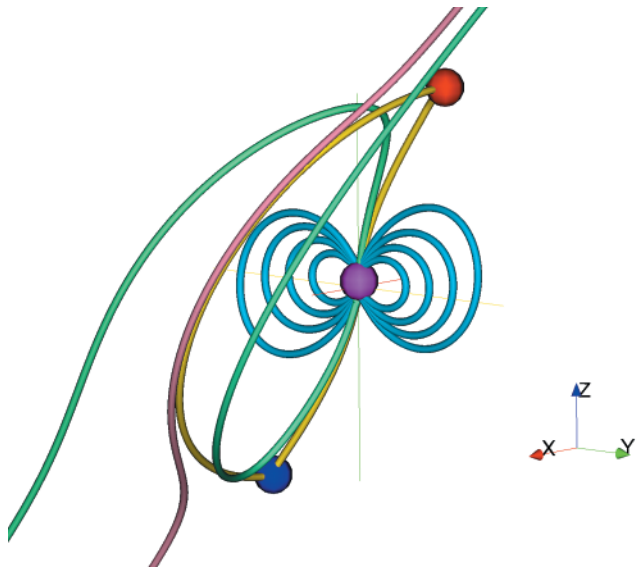

Figure 8. In three dimensions a particular solar wind field line does not, in general, make contact with northern and southern tail lobe field lines simultaneously. As *Russell* [1972] notes, solar wind field lines which make contact with tail lobe field lines in one hemisphere will transform into open field lines which drape over the dayside magnetosphere in opposite senses on the dawn and dusk sides of the magnetosphere (green tubes in the figure). Nevertheless, in the vacuum superposition topology shown here, there is, for any IMF orientation, a single field line which joins the two cusp null points. Though one can interpret this closed field line as a solar wind field line (shown in red) which makes contact with the two cusp nulls simultaneously, one cannot, from inspection of the magnetic field topology alone, identify magnetic reconnection as a local process occurring at the nulls.

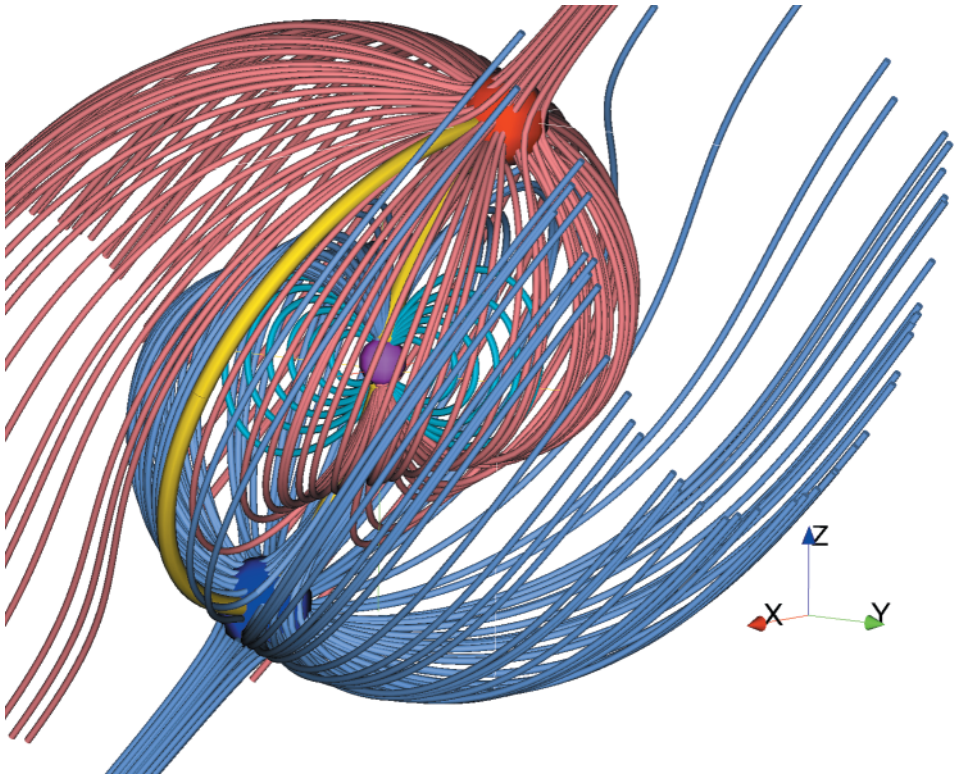

Figure 9. This figure illustrates Dungey's vacuum superposition topology under generic northward IMF conditions. In general, the spherical separatrix surface of Figure 7 breaks up into two distinct surfaces, illustrated here by two sets of magnetic field streamlines: (1) red lines which pass through the northern cusp null (red sphere), (2) blue lines which pass through the southern cusp null (blue sphere). The intersection of the two surfaces defines a separator loop, consisting of two separator lines which join the northern null to the southern null (the yellow tube is a closed field line which shows the approximate location of one of these separators). Note that there are now three topologically distinct classes of field lines: (1) solar wind field lines (extending to infinity in both directions), (2) open field lines (extending to infinity in one direction and intersecting the central purple sphere in the other), (3) closed field lines (intersecting the purple sphere in both directions).

yellow field line is identified as the separator line since it is defined by the intersection of the two separatrix surfaces.

[15] The separator line of Figure 9 is the three-dimensional analogue of the two-dimensional X lines of Figure 3, but whereas there are two distinct separator lines in the two-dimensional case, there is only one in the three-dimensional case. Further, just as the reconnection electric field at a two-dimensional null line is (by definition) not localized at one particular position on the line, the parallel electric field at a three-dimensional separator line is not, in general, localized at a particular position on the separator line (e.g., near a null point). This presents a problem in three dimensions, since one cannot determine, from the magnetic topology alone, the spatial distribution of the parallel electric field. Is the parallel electric field concentrated around the magnetic nulls or at some other location along the separator line? To what extent do magnetic nulls and separator lines constrain the dynamics of reconnection in three dimensions (as they clearly do in two dimensions)? Can an arbitrary, locally hyperbolic field line (i.e., a line with the property that the magnetic field projected onto the planes perpendicular to the line has a hyperbolic null) play the role of a reconnection X line in three dimensions? Addressing such questions requires one to move beyond magnetic topology and address the geometry of the magnetic field: How is current density distributed on the magnetopause surface? Traditionally, there have been two competing hypothetical answers to this question, both of which are motivated by two-dimensional magnetic reconnection theory: (1) the component reconnection hypothesis and (2) the antiparallel reconnection hypothesis. In the following section we review observations and theoretical models which support both of these hypotheses. While a number of the models reviewed below are kinetic models, in this work we address the component/antiparallel reconnection issue in the context of resistive MHD. While resistive MHD is incapable of addressing the reconnection timescale problem (i.e., the strong scaling of the reconnection rate with plasma resistivity), it is currently the only model which is capable of addressing the global three-dimensional geometry of the dayside magnetopause X line; indeed, our resistive MHD calculations demonstrate that the component and antiparallel hypotheses are not mutually exclusive in a global three-dimensional magnetosphere.

1.3. Component Reconnection Hypothesis

[16] Component reconnection at the dayside magnetopause was originally treated by *Sonnerup* [1974] as a

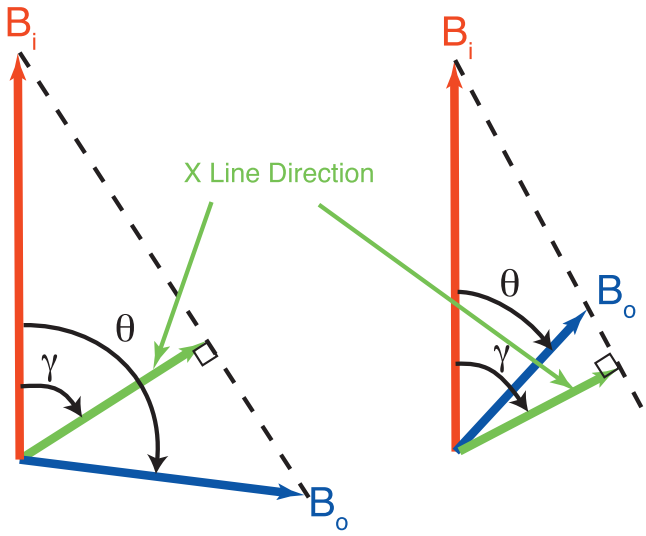

Figure 10. This figure illustrates the geometry of component reconnection, viewed from the Sun. Red arrows labeled "B_i" show the magnetospheric magnetic field; blue arrows labeled "B_o" show the magnetosheath magnetic field. The left figure shows a case where reconnection is geometrically possible, according to the Sonnerup criterion. The right figure shows a case where reconnection is precluded by the Sonnerup constraint (i.e., the projection of the magnetic field in the plane perpendicular to the average current in the sheet has no hyberbolic null).*

generalization of two-dimensional "guide field" reconnection, in which reconnection along a two-dimensional hyperbolic neutral line is modified by the addition of a constant background field parallel to the neutral line. Since the current density is directed along the neutral line in such models, *Sonnerup* [1974] suggested that one should identify the X line at the magnetopause current sheet with the direction of the integrated (across the sheet) current density (Figure 10). Since the magnetic field on the magnetosheath side of the current sheet is typically weaker than that on the magnetosphere side, *Sonnerup* [1974] argued that magnetic reconnection would be geometrically impossible whenever the clock angle, θ, of the magnetosheath field is less than $\cos^{-1}(B_o/B_i)$ (here, B_o is the "outer" magnetosheath field, and B_i is the "inner" magnetospheric field). *Cowley* [1976], however, pointed out that the magnitude of the guide field may vary arbitrarily across the current sheet (as described, for example, by *Sonnerup and Priest* [1975]), making the identification of a unique X line direction, e.g., parallel to the direction of the integrated current, problematic. If the component of the magnetic field parallel to the X line can vary arbitrarily across the current sheet, then the angle between the X line and B_i can, in principle, range from 0 to θ, the X line need not be parallel to either the current density or the integrated current (as is the case in two-dimensional, constant guide field reconnection). Thus there seems to be no a priori objection to the possibility that subsolar reconnection is possible for all nonvanishing θ.

[17] The arguments of *Cowley* [1976] raise an interesting question: How low must the magnetic shear at the subsolar magnetopause be before magnetic reconnection is geometrically precluded? Spacecraft observations have not yet provided an unambiguous answer to this question. *Gosling et al.* [1982] presented indirect evidence, observations of fast magnetopause flows (consistent with acceleration at rotational discontinuities) by the ISEE 1 and 2 spacecraft, of magnetic reconnection for magnetic shear angles less than 90°. *Gosling et al.* [1990] even observed so-called "flow reversal events," in which the magnetopause stagnation flow field is distorted by the motions of newly reconnected flux tubes, for cases where the magnetic shear was as low as 50°. While *Paschmann et al.* [1993] observed, with the AMPTE/IRM spacecraft, evidence of plasma transport from the magnetosheath into the magnetosphere at the low shear (where the field rotated by less than 30° from the magnetosheath to the magnetosphere) magnetopause, such plasma entry was interpreted as either a "nonreconnection transfer process" or a consequence of high-latitude reconnection at one of the cusp nulls. Indeed, the AMPTE/IRM data analysis presented by *Paschmann et al.* [1993] suggests that the changes in plasma conditions associated with low-latitude, low-shear magnetopause crossings, bulk velocity direction, plasma temperature, and temperature anisotropies, are not, in general, accompanied by a clear rotation of the magnetic field. Nevertheless, evidence of reconnection equatorward of the polar cusp under northward IMF conditions has been found in AMPTE/CCE [*Fuselier et al.*, 1997], Polar-TIDE [*Chandler et al.*, 1999], and Polar-TIMAS [*Fuselier et al.*, 2000] magnetopause crossings (though *Russell and Le* [2000] interpret the Polar-TIMAS component reconnection case study [*Fuselier et al.*, 2000] as a case of antiparallel reconnection tailward of the cusp).

1.4. Antiparallel Reconnection Hypothesis

[18] In contrast to the component reconnection hypothesis, the antiparallel reconnection hypothesis posits that magnetopause reconnection is localized around regions where the magnetosheath and magnetospheric magnetic fields are antiparallel [*Crooker*, 1979]. "Antiparallel" is usually defined in the context of a magnetic field model [e.g., *Tsyganenko*, 1995a; *Tsyganenko and Stern*, 1996] for which the magnetopause surface, separating the solar wind magnetic field from the magnetospheric magnetic field, is unambiguously defined. The X line is then identified with the locus of points on the magnetopause for which the magnetic field vectors on either side of the surface point in opposite directions (i.e., θ_c = 180° in Figure 10). While component reconnection was initially motivated [*Sonnerup*, 1974] by the two-dimensional theory of driven guide field reconnection, the antiparallel construction is similar in spirit to a tearing mode calculation in which one assesses the tendency of an initial current sheet (for which the component of the magnetic field normal to the sheet vanishes) to undergo magnetic reconnection. Indeed, the linear tearing mode analysis of *Quest and Coroniti* [1981], which demonstrates that the growth rate scales inversely with the magnitude of the guide field, provided early theoretical motivation for antiparallel reconnection. A recent linear analysis of three-dimensional resistive tearing, however, suggests that it is not appropriate (or even meaningful) to compute two-dimensional tearing mode growth rates at separate locations on the magnetopause surface [*Hu et al.*,

*The caption is correct here. The article as originally published is online.

2004]. In the *Hu et al.* [2004] analysis, an initially closed magnetic field topology equivalent to that of Figure 7 becomes open due to resistive tearing of the spherical separatrix surface which carries the confining current. The breakup of the spherical tearing surface is associated with a parallel electric field which is not localized around the magnetic nulls. In contrast, the *Quest and Coroniti* [1981] analysis predicts that the tearing mode growth rate should have local maxima at the antiparallel loci which, by definition, contain the magnetic nulls.

[19] In two dimensions the presence of a significant guide field can suppress nonlinear reconnection for a number of reasons. *Rogers et al.* [2001], for example, argues that the dispersive properties of whistler and kinetic Alfvén waves facilitate fast reconnection by preventing the collapse of X type neutral lines into macroscopic Sweet-Parker sheets. Therefore if the guide field is large enough to suppress such waves, then one expects an associated reduction in the reconnection rate. *Rogers et al.* [2001] observed such a reduction in two-fluid simulations of nonlinear reconnection starting from a double Harris sheet equilibrium (in which electron inertia breaks the frozen flux constraint). Using a two-dimensional electromagnetic particle-in-cell (PIC) code, *Swisdak et al.* [2003] demonstrate that the presence of a guide field, in combination with a density gradient normal to the reconnection plane, can suppress reconnection by inducing a diamagnetic electron drift which convects the X line at a speed exceeding the Alfvén speed. Using a three-dimensional electromagnetic PIC code, *Tanaka et al.* [2004] show that rapid triggering of the tearing mode instability in a Harris equilibrium (associated with the fast growing lower hybrid drift instability at the edges of the current sheet) is suppressed in the presence of a guide field. *Karimabadi* [2005] argues that if tearing at the dayside magnetopause is enhanced by its coupling with the Weibel instability [*Weibel*, 1959] (which is driven by electron temperature anisotropies induced by lower hybrid fluctuations at the edges of the current sheet [*Daughton et al.*, 2004]), then fast tearing may be suppressed by the presence of a guide field which suppresses the Weibel instability; nevertheless, *Karimabadi* [2005] also find in their hybrid simulations that fast, steady state reconnection is possible for moderately large magnitudes of the guide field (of the order of the reconnecting field components).

[20] The observational support for the antiparallel hypothesis can be roughly categorized as follows: (1) in situ observations of fast plasma flows and particle velocity distributions which provide some information about the location of the observing spacecraft relative to the reconnection site; (2) remote sensing of ionospheric signatures of reconnection at the magnetopause. Evidence in the first category is usually in the form of Alfvénic plasma flows and D-shaped ion velocity distributions [*Cowley*, 1982] indicating plasma acceleration across rotational discontinuities [*Gosling et al.*, 1991; *Kessel et al.*, 1996; *Russell et al.*, 1998; *Fuselier et al.*, 2000; *Le et al.*, 2001; *Onsager et al.*, 2001; *Scudder et al.*, 2002; *Lavraud et al.*, 2002; *Phan et al.*, 2003; *Trattner et al.*, 2004]. Most such in situ evidence seems to be associated with northward IMF conditions (the *Gosling et al.* [1991] study is a rare exception in which the IMF was weakly southward); this is consistent with the notion that magnetic reconnection is a local process associated with the magnetic neutral points in the *Dungey* [1961, 1963] model. We note, however, that not all evidence of high-latitude (poleward of the cusp) reconnection under northward IMF conditions is consistent with the notion that reconnection is strongly localized around the antiparallel locus. For example, the *Trattner et al.* [2004] analysis considered two distinct events in which the Polar spacecraft crossed the cusp under northward IMF conditions. In one event (22 September 1997), the location of the reconnection site, inferred from a time-of-flight analysis of ion velocity distributions observed by the TIMAS instrument, was consistent with antiparallel merging. In the second event (30 October 1997), however, the time-of-flight analysis yielded a reconnection location which, though located at high latitude, was associated with a magnetic shear angle of about 100°. Nevertheless, *Trattner et al.* [2004] interpret this discrepancy as evidence that the high-latitude X line, while originating at the antiparallel locus, extends some significant distance away from the locus.

[21] Observations in the second category, remote sensing of ionospheric signatures of magnetopause structure, have produced conflicting results. Using data from the Super Dual Auroral Radar Network (SuperDARN), *Coleman et al.* [2001] observe ionospheric convection patterns which, they argue, are consistent with a bifurcated magnetopause X line under southward IMF conditions. *Petrinec and Fuselier* [2003], however, argue that the ionospheric gap in the mapped magnetopause antiparallel locus predicted by *Coleman et al.* [2001] is associated with inaccuracies in the numerical methods used to map field lines (namely, errors associated with tracing field lines near magnetic nulls as well as poor resolution of field line seed points). Indeed, *Fuselier et al.* [2002] has shown evidence from one of the imagers aboard the IMAGE (Imager for Magnetopause to Aurora Global Exploration) spacecraft that a proton auroral spot observed poleward of the auroral oval maps to the antiparallel locus on the magnetopause surface (both the mapping and the magnetopause surface were defined by the T96 Tsyganenko model [*Tsyganenko*, 1995b, 1996]. The spot, *Fuselier et al.* [2002] argue, is produced by Lyman alpha emission from $\sim$1 keV protons which, having been energized by magnetic reconnection poleward of the cusp under northward IMF conditions, undego charge exchange in the upper atmosphere to become excited neutral hydrogen. In contrast, under southward IMF conditions, *Fuselier et al.* [2002] argue that proton auroral emissions associated with magnetic reconnection map to the subsolar magnetopause. Recent simultaneous observations by the Cluster and IMAGE spacecraft show that under northward IMF conditions, the usual in situ (Cluster) signatures of reconnection poleward of the cusp, namely, bulk velocity acceleration satisfying the Walén test), mapped along magnetic field lines (using various versions of the Tsyganenko model) to the proton auroral spot observed by IMAGE [*Phan et al.*, 2003].

1.5. What Have We Learned From Simulations?

[22] Given the ambiguities and contradictions present in many of the spacecraft observations, global three-dimensional simulation of Earth's magnetopause is an essential tool for the investigation of the geometry of dayside magnetopause reconnection. Unfortunately, despite

the fact that the magnetosphere is a nearly collisionless plasma which is far from local thermodynamic equilibrium, computational resources have not yet reached a level which makes possible global three-dimensional kinetic (e.g., PIC) simulations of the magnetopause. Resistive MHD simulation is still the preferred approach, despite its well-known limitations (in particular, its inability to model fast reconnection in the high Lundquist number limit [*Dorelli et al.*, 2004]).

[23] What, then, have resistive MHD simulations taught us about the geometry of the dayside magnetopause X line? Over the last decade, a number of global MHD simulation studies have provided evidence that the magnetospheric magnetic field topology is consistent in many respects with the vacuum superposition topology originally envisioned by Dungey. *Fedder et al.* [1995] investigated the dependence of the magnetotail topology on the IMF; while the magnetic field topologies shown in their Plate 2 show evidence of a global separator structure (which *Fedder et al.* [1995] identify as the intersection of the magnetopause with the surface separating IMF field lines from open field lines), it is not clear whether or not this separator is related to the separator line which joins the two magnetic nulls in the generic vacuum superposition topology shown in Figure 7. *Russell et al.* [1998] compare magnetic field data from the Polar mission with results from a global MHD simulation, arguing that under the sustained northward IMF conditions which occurred from 0230 to 0800 on 29 May 1996 the simulated magnetic field topology was consistent with Dungey's pure northward IMF topology (Figure 7), in which magnetosheath plasma is captured onto closed field lines by simultaneous reconnection at the two cusp nulls. The nulls were not tracked in the simulations, however. Figure 5 of *Russell et al.* [1998] shows a noon-midnight meridional projection of the magnetic field topology; nevertheless, given the fact that separatrices in two-dimensional projections need not coincide with three-dimensional separatrices, it is not clear whether (1) there is a single closed surface separating closed from open field lines, and (2) whether plasma is flowing across such a separatrix (a necessary condition for the occurrence of simultaneous cusp reconnection). Similar simulation evidence of simultaneous cusp null reconnection under sustained northward IMF conditions was presented more recently by *Le et al.* [2001] and *Li et al.* [2005]; again, however, no attempt was made to track (in the simulation data) three-dimensional topological properties of the magnetic field (magnetic nulls, separatrix surfaces, and separator curves).

[24] A number of global MHD simulation studies of magnetopause merging in the last decade have been interpreted in the context of the vacuum superposition topology. *Crooker et al.* [1998] explained lobe cell ionospheric convection (in which the convection cell is confined to the open polar cap) as a consequence of electric potential drops along open magnetic field lines which "overdrape" across the dayside magnetopause, threading a broad diffusion region on the dayside magnetopause as they converge toward two cusp nulls (one in each hemisphere). The vacuum superposition topology, in which a separator line extends from the southern to the northern cusp null, was invoked to motivate the existence of these "newly reconnected" overdraped field lines. A similar magnetic field topology was found in the simulations of *Tanaka* [1999] and *Watanabe et al.* [2004], though their interpretation of the relationship between ionospheric convection patterns and magnetopause reconnection under northward IMF conditions differs from that of *Crooker et al.* [1998] (who considered the case where the z component of the magnetic field in GSM coordinates vanishes). Considering a pure duskward IMF case, *Siscoe et al.* [2001] identify two magnetic nulls and a separator line joining the two nulls, demonstrating that the parallel electric field is weaker at the nulls than at the subsolar point (by about a factor of three). *Siscoe et al.* [2001] thus infer that reconnection under duskward IMF conditions bears more resemblance to component reconnection than to antiparallel reconnection.

[25] One can organize the results summarized in the previous two paragraphs (our citations are by no means an exhaustive list) into two categories of models: (1) models which treat magnetic reconnection as a local process, analogous to two-dimensional reconnection at an X line, and possibly associated with a magnetic null (representative models include *Russell et al.* [1998]; *Tanaka* [1999]; *Le et al.* [2001]; *Li* [1999]; *Watanabe et al.* [2004]); (2) models which treat magnetic reconnection as an inherently global process, involving three-dimensional separatrix surfaces the intersections of which define global separator lines [e.g., *Fedder et al.*, 1995; *Crooker et al.*, 1998; *Siscoe et al.*, 2001]. Models in the first category visualize the reconnection process as a local "breaking" and "rejoining" process analogous to that which one associates with a two-dimensional X type neutral point. In contrast, models in the second category view the reconnection process as a global process which occurs at a rate which is given by a line integral (perhaps along a separator line) of the parallel electric field. Interestingly, a number of the models described in this subsection [*Tanaka*, 1999; *Watanabe et al.*, 2004; *Crooker et al.*, 1998; *Siscoe et al.*, 2001] fall into separate categories (local versus global reconnection) despite the fact that they explicitly interpret the simulation results in the context of the same separator reconnection topology, in which three-dimensional separatrix surfaces intersect at separator lines joining isolated magnetic nulls. This is not surprising, given that one cannot determine, from the magnetic field topology alone, the spatial distribution of the parallel electric field on the magnetopause surface. To our knowledge, *Siscoe et al.* [2001] is the first attempt to identify magnetic reconnection with the parallel electric field along a separator line in a global MHD simulation of the magnetosphere.

[26] In this paper we revisit the problem of determining the topology and geometry of dayside magnetopause magnetic reconnection under northward IMF conditions. Whereas *Siscoe et al.* [2001] considered a zero dipole tilt case in which the IMF points in the duskward direction, we consider a generic northward IMF case, with zero dipole tilt and an IMF clock angle of 45°. We address the following questions:

[27] 1. What is the topology of the dayside magnetopause magnetic field under generic northward IMF conditions? What is the role of magnetic nulls, and associated separatrix surfaces, in constraining the dynamics of magnetopause magnetic reconnection?

[28] 2. What is the geometry of the dayside X line? Does the X line correspond to the antiparallel locus or does it extend across the subsolar region?

[29] 3. How is the parallel electric field distributed on the magnetopause surface? Can magnetic reconnection be viewed as a local process, with a spatially localized diffusion region, or is magnetopause reconnection an inherently global process, with the reconnection rate determined by a line integral of the electric field?

2. Results

2.1. OpenGGCM Model

[30] The results presented in this paper were obtained using the OpenGGCM (Global Geospace Circulation Model) code, a resistive MHD code which is maintained at the Institute for the Study of Earth, Oceans, and Space (EOS) at the University of New Hampshire (UNH). OpenGGCM is a finite difference code (originally developed by J. Raeder; see, for example, [*Raeder et al.*, 1995; *Raeder*, 2003]) which computes the interaction of the solar wind with Earth's magnetosphere. The code is parallelized, using the message passing interface (MPI), to run on massively parallel computing architectures. The computations were performed on a 340 processor Beowulf cluster (Zaphod) at EOS.

[31] In the outer magnetosphere (outside a sphere of radius 3.5 R_E centered around Earth), the normalized resistive MHD equations are solved using explicit finite difference schemes (to be described below):

$$\frac{\partial \rho}{\partial t} = -\nabla \cdot (\rho \mathbf{U}) \tag{4}$$

$$\frac{\partial \rho \mathbf{U}}{\partial t} = -\nabla \cdot (\rho \mathbf{U}\mathbf{U} + p\mathbf{I}) + \mathbf{J} \times \mathbf{B} \tag{5}$$

$$\frac{\partial u}{\partial t} = -\nabla \cdot [(u + p)\mathbf{U}] + \mathbf{J} \cdot \mathbf{E} \tag{6}$$

$$\frac{\partial \mathbf{B}}{\partial t} = -\nabla \times \mathbf{E} \tag{7}$$

$$\nabla \cdot \mathbf{B} = 0 \tag{8}$$

$$\mathbf{E} = -\mathbf{U} \times \mathbf{B} + \frac{1}{S}\mathbf{J} \tag{9}$$

$$\nabla \times \mathbf{B} = \mathbf{J} \tag{10}$$

$$u = \frac{1}{2}\rho U^2 + \frac{p}{\gamma - 1} \tag{11}$$

where $\mathbf{I}$ is the unit tensor and γ is the ratio of specific heats. The variables are dimensionless, having been normalized as follows: spatial coordinates are normalized by $1R_E$; the plasma density, ρ, is normalized by a reference value, $\rho_0 = 10^4$ cm^{-3}; the magnetic field, $\mathbf{B}$, is normalized by the magnitude of Earth's dipole field at 1 R_E; the bulk velocity, $\mathbf{U}$, is normalized by the reference Alfvén speed, $V_A = B_0/(4\ \pi\ \rho_0)^{1/2}$; the plasma pressure, p, and energy density, u, are normalized by the reference magnetic energy density, $B_0^2/(8\ \pi)$; t is normalized by the Alfvén time, $t_A = \lambda/V_A$ (where $\lambda = 1\ R_E$); the current density, $\mathbf{J}$, and the electric field, $\mathbf{E}$, are normalized so that equations (9) and (10) are satisfied. The Lundquist number, S, is constant in time and spatially uniform (save for a spherical region of radius 6 R_E around Earth, where the resistivity is set to zero). The reader should note that S is defined here in terms of the reference magnetic field at 1 R_E, as well as the reference density of 10^4 cm^{-3}. Thus the Lundquist number defined in terms of magnetosheath parameters, with a magnetic field of about 50 nT, a density of about 30 cm^{-3}, and a scale of a few Earth radii, gives a magnetosheath Lundquist number, S_{MS}, of approximately $S/10$.

[32] Equations (4)–(11) are solved on a nonuniform rectilinear grid in GSE coordinates. In the y and z dimensions the grid is exponential, extending out to $\pm 40\ R_E$, with a minimum grid spacing of 0.1 R_E at $y = z = 0$, at the subsolar point, and a maximum grid spacing of 0.5 R_E at $\pm 40\ R_E$. In the x direction, the grid extends from 24 R_E on the dayside to 200 R_E in the tail; the grid is again nonuniform, with grid points concentrated around the dayside magnetopause, where the resolution is $\approx 0.025\ R_E$. We have performed convergence tests to verify that the magnetopause reconnection physics we describe in subsequence sections is not sensitive to the grid resolution (though we do not yet have the computational resources to investigate global convergence for the Lundquist number, $S = 5000$, used in this study). The simulation resolution is such that the magnetopause current sheet is well resolved over most of the dayside magnetopause surface.

[33] As discussed by *Raeder* [1999], the gasdynamic part of the MHD equations, equations (4)–(6), are spatially discretized using a hybrid scheme in which fourth-order centrally differenced fluxes are combined with first-order Rusanov fluxes (with the high-order fluxes dominating in smooth regions), while Faraday's law, equation (7), is discretized using the constrained transport method developed by *Evans and Hawley* [1988] (this method preserves the constant (8) to machine precision). All of the equations are advanced in time using a second-order predictor-corrector scheme. The boundary conditions on the dayside are fixed in time, while those on the other five boundaries are free (i.e., normal derivatives vanish).

[34] Field-aligned currents (FAC), $J_{||}$, are computed just outside a spherical region of radius 3.5 R_E, centered around Earth, and mapped to a spherical-polar ionosphere grid at 1 R_E using a dipole magnetic field model. The mapped FAC are used to compute the source term in the current continuity equation:

$$\nabla \cdot \Sigma \cdot \nabla \Phi = -J_{\parallel} \sin I \tag{12}$$

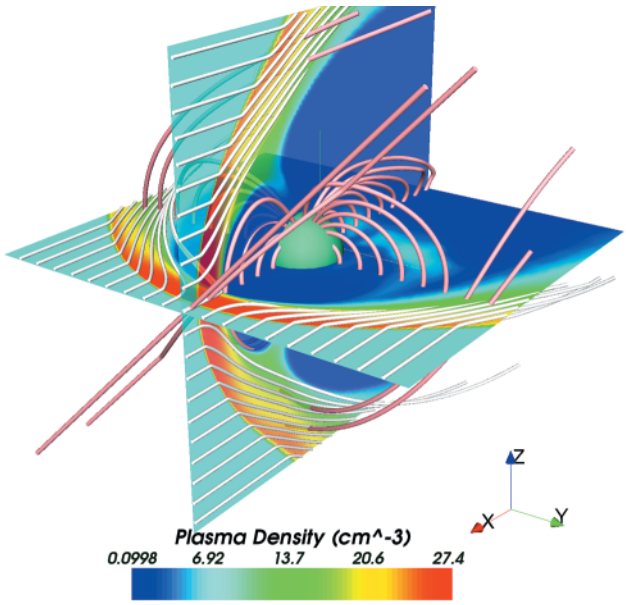

Figure 11. This figure shows a global view of the interaction of the solar wind with Earth's magnetosphere, simulated by the OpenGGCM model. Earth is the blue sphere in the center. The two cut planes show plasma density; the bow shock is clearly visible as the sharp increase (green-red transition) in plasma density, and the dayside magnetopause can be clearly identified, in the subsolar region, as the sharp density drop. White tubes show bulk plasma streamlines, while colored tubes show magnetic field streamlines (color coded according to the magnetic field magnitude). The solar wind conditions for this run were steady, with an IMF clock angle of 45°.

where Φ is the ionospheric potential on a spherical grid at 1 AU, $\boldsymbol{\Sigma}$ is a conductivity tensor, and I is the inclination of the dipole field at the ionosphere. Equation (12) is solved using a Galerkin pseudospectral method on a spherical-polar grid, with the boundary condition $\Phi = 0$ at the equator. The ionospheric conductivities include contributions from EUV ionization, diffuse auroral electron precipitation, and discrete aurorae associated with parallel electric fields (see *Raeder et al.* [2001] for details).

[35] In what follows, we analyze results from a single run (used to produce Figure 11), corresponding to an IMF clock angle of 45. The dipole tilt is zero, and the following steady solar wind boundary conditions are used: the IMF B_y and B_z are both 5 nT; the solar wind speed is 400 km/s; the solar wind density is 5 cm^{-3}; the solar wind pressure is 7 pPa. The code was run long enough for a steady state to be reached on the dayside (typically this requires approximately 15 min of simulated time, though we run the simulation for 2 hours of simulated time). The Lundquist number, S, was set to 5000.

2.2. Tracking Magnetic Nulls in the OpenGGCM Simulation

[36] We make use of an algorithm developed by *Greene* [1992] to track magnetic nulls in the simulation. Greene's algorithm is based on the concept of the topological degree of a map f: $R^n \rightarrow R^n$, relative to the domain $D \subseteq R^n$. The map f takes the vector $\mathbf{x} = \langle x_1, x_2, \ldots, x_n \rangle$ to the vector $\mathbf{f} = \langle f_1(\mathbf{x}), f_2(\mathbf{x}), \ldots, f_n(\mathbf{x}) \rangle$. Let $\mathbf{J}_f$ be the Jacobian of f. Then the topological degree [*Kronecker*, 1869] of f, relative to domain D, is defined as

$$deg(f, D) = \sum_{x \in f^{-1}(\mathbf{0})} sgn\left[det\left(\mathbf{J}_f(x)\right)\right] \tag{13}$$

where $\mathbf{0}$ is the n-dimensional zero vector. Thus the topological degree is the difference between the number of solutions of $\mathbf{f} = \mathbf{0}$ for which $det(\mathbf{J}_f(x)) > 0$ and the number for which $det(\mathbf{J}_f(x)) < 0$. In other words, the topological degree counts the difference between the number of type A nulls and the number of type B nulls within D. One can compute the topological degree by evaluating the Kronecker integral [see, e.g., *Polymilis et al.*, 2003]:

$$deg(f, D) = \frac{\Gamma(n/2)}{2\pi^{n/2}} \int_{\partial D} \frac{\sum_{i=1}^{n} A_i dx_1 \ldots dx_{i-1} dx_{i+1} \ldots dx_n}{\left(f_1^2 + f_2^2 + \cdots f_n^2\right)^{n/2}} \tag{14}$$

where $\Gamma(x)$ is the gamma function and

$$A_i = (-1)^{n(i-1)} det(\mathbf{M}) \tag{15}$$

$\mathbf{M}$ is the n by n matrix such that $M_{i1} = f_i$ and $M_{ij+1} = \frac{\partial f_i}{\partial x_j}$ with j ranging over $\{1, \ldots, i-1, i+1, \ldots, n\}$.

[37] For example, when the map in question is the magnetic field, $\mathbf{B}$, the Kronecker integral takes the following form:

$$deg(\mathbf{B}, D) = \frac{1}{4\pi} \int_{\partial D_B} \frac{\mathbf{B} \cdot d\boldsymbol{\sigma}}{B^3} \tag{16}$$

where we have transformed the integral into magnetic field space, D_B is the image of D under the map $\mathbf{B}(\mathbf{x})$, $d\sigma$ is a differential surface element in magnetic field space, and B is the magnitude of the magnetic field (B is the distance from the origin in magnetic field space).

[38] By Gauss' Law, if ∂D_B encloses the origin once (i.e., if ∂D contains a single magnetic null), then $deg(B, D) = \pm 1$ (the sign is determined by the orientation of ∂D_B, which is, in turn, determined by the map $\mathbf{B}$ from D to D_B). Similarly, if D contains N nulls, then one can break up (16) into a sum of integrals, each one corresponding to a subvolume, D_s, enclosing a single null.

[39] *Greene* [1992] discretizes (16) by sampling magnetic field vectors on D, triangulating the sampled points (see Figure 12), transforming the resulting triangles into magnetic field space (thus approximating ∂D_B by the polyhedron $\partial \tilde{D}_B$ in magnetic field space; see the right panel of Figure 12), and computing the following sum:

$$deg(\mathbf{B}, D) \approx \sum_{i=0}^{N_T} A_i \tag{17}$$

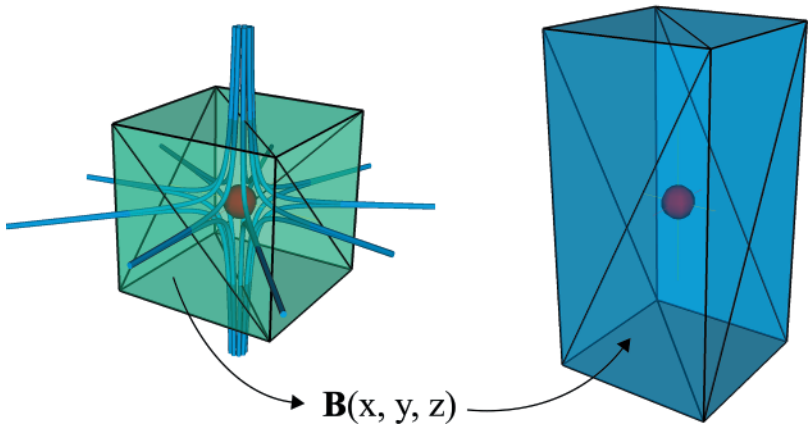

Figure 12. This figure illustrates the calculation of the topological degree of a discretized magnetic field, relative to an OpenGGCM finite difference cell. Each computational cell is decomposed into 12 triangles (green cube), each of which is mapped (using the values of the magnetic field at the eight vertices of the cell) to a corresponding triangle in magnetic field space (blue cube). In this example there is a single linear null (red sphere) such that $B_x = x$, $B_y = y$ and $B_z = -2z$.

where N_T is the number of triangles, and

$$A_i = 4\tan^{-1}\{[\tan(\theta_1+\theta_2+\theta_3)/4 \times \tan(\theta_1+\theta_2-\theta_3)/4 \times \tan(\theta_2+\theta_3-\theta_1)/4 \times \tan(\theta_3+\theta_1-\theta_2)/4]^{1/2}\} \quad (18)$$

A_i is the area of the spherical triangle corresponding to the projection of the ith triangle of $\partial\tilde{D}_B$ onto the unit sphere in magnetic field space: $\cos\theta_i = (\mathbf{B}_j \cdot \mathbf{B}_k)/|\mathbf{B}_j||\mathbf{B}_k|$, where the indices $\{i, j, k\}$ are cyclic permutations of $\{1, 2, 3\}$. The areas of the spherical triangles are oriented such that A_i has the same sign as the volume element $\mathbf{B}_i \cdot \mathbf{B}_j \times \mathbf{B}_k > 0$.

2.3. Simulated Vacuum Superposition Topology

[40] Figure 13 shows a cut of the OpenGGCM simulation in the GSE $z = 0$ plane, illustrating magnetic flux pileup and associated plasma depletion under generic northward IMF conditions. The top panel shows the magnetic field magnitude; the bottom panel shows the plasma pressure. Green arrows show the projection of the plasma bulk velocity vectors into the plane. The two purple lines show the locations where the two magnetic separatrix surfaces (separating solar wind, open and closed field lines) intersect the GSE $z = 0$ plane. We identify the subsolar magnetopause with the intersection of these two purple lines, which occurs at $X_{GSE} \approx 10.35\ R_E$ (note the "double Y" topology of the projected separatrices, reminiscent of two-dimensional Sweet-Parker reconnection).

[41] Although Figure 13 is a snapshot taken after 6840 s of simulated time (this time step was chosen randomly), the dayside magnetosheath and magnetopause are remarkably steady during the 2 hours of simulated time. Figure 14 demonstrates the steadiness of the magnetopause location and current density. The blue dots show the subsolar magnetopause location, defined to be location, along the Sun-Earth line, of the local maximum of the current density, as a function of time. After an initial transient phase lasting about 1000 s (and associated with the fact that the initial condition is not a static equilibrium), the dayside magnetopause settles into a steady state which persists until the end of the simulation, after 7200 s of simulated time. The green dots show the current density at the subsolar magnetopause, demonstrating that there is a significant and steady reconnection electric field at the subsolar magnetopause under generic northward IMF conditions. As we will see later, this current density is associated with a thin current sheet which forms near a magnetic separator line which extends across the subsolar magnetopause, terminating in the polar cusps.

[42] Figure 15 shows the magnetic skeleton computed from the OpenGGCM simulation after 6840 s of simulated time. The red lines in the figure are magnetic field streamlines corresponding to 180 seed points randomly distributed within spheres of radius 1.5 R_E around the northern cusp null (marked "A") located at the point $N_1 = (-2.4\ R_E, 6.3\ R_E, 12.9\ R_E)$. Likewise, the blue lines are streamlines with seed points within a 1.5 R_E radius of the southern cusp null (marked "B") located at the point $N_2 = (-3.2\ R_E, -6.5\ R_E, -13.5\ R_E)$. Thus the blue and red field lines lie approximately on the Σ surfaces associated with the two nulls. The yellow line is the magnetic field streamline which passes through the point (10.35 R_E, 0 R_E, 0 R_E), the approximate location of the magnetopause along the Sun-Earth line. Note that this line passes very close to the two nulls used to visualize the Σ surfaces. Also note that the two Σ surfaces come into contact at the approximate location of the yellow field line. Thus the yellow line gives the approximate location of the magnetic separator defined by the intersection of the two separatrix surfaces associated with nulls N_1 and N_2.

[43] It is clear from Figure 15 that the topology of the simulated magnetopause is more complex than that of the simple vacuum superposition. While the vacuum superposition topology has two magnetic nulls, a single type A null and a single type B null, the topology shown in Figure 15 has more than two magnetic nulls. Indeed, there appear to be four distinct clusters of magnetic nulls, two in the

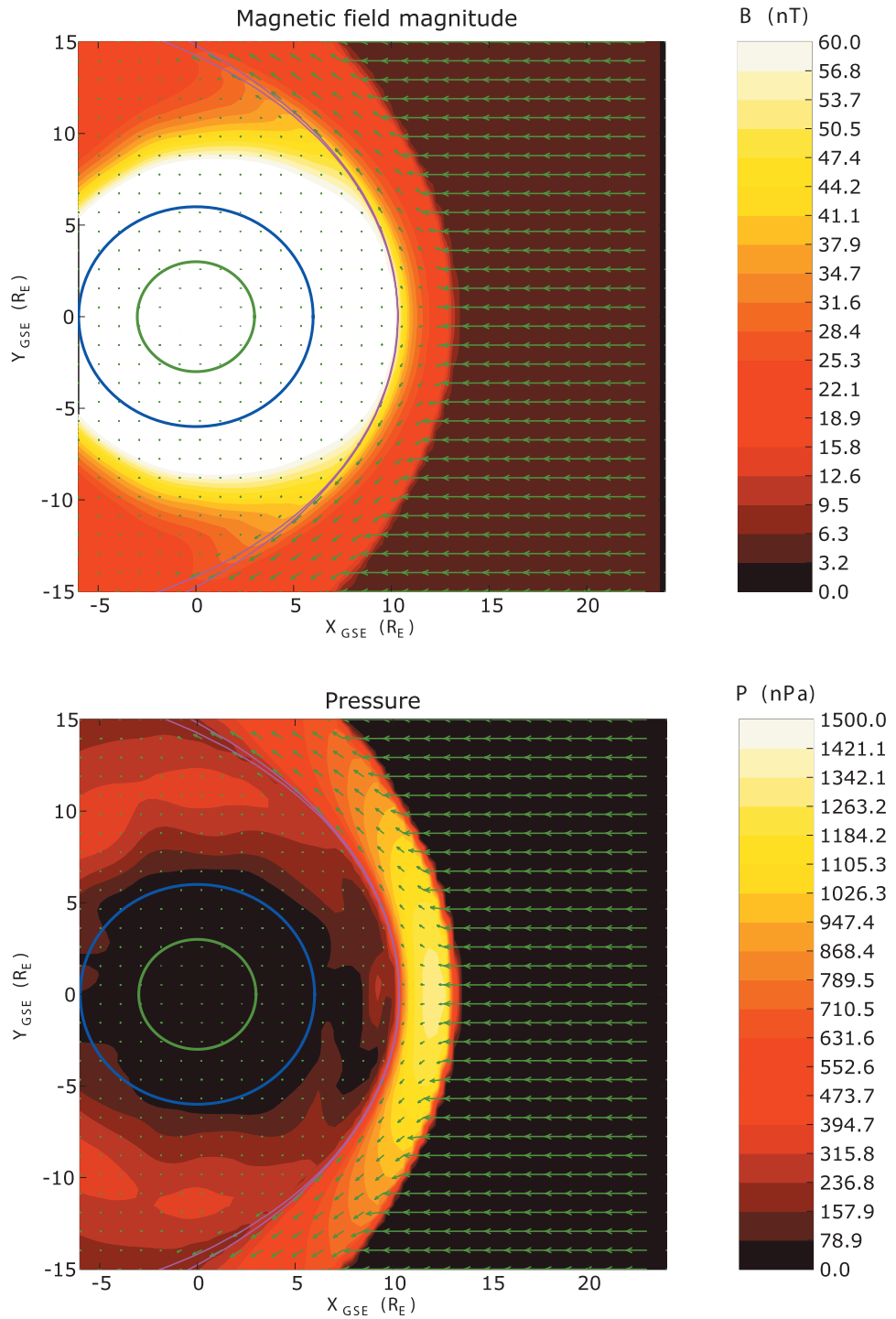

Figure 13. This figure illustrates (top) magnetic flux pileup and (bottom) associated plasma depletion upstream of Earth's dayside magnetopause under generic northward IMF conditions. Green arrows show the bulk velocity projected into the plane. The purple lines show the intersections of the solar wind/open and open/closed magnetic separatrix surfaces with the plane (note the "double Y" topology, reminiscent of Sweet-Parker reconnection). The green circle is the inner MHD boundary condition, where field aligned currents are mapped to the ionosphere; the blue circle is the inner resistivity boundary, within which the resistivity is set to zero. The plasma resistivity is constant everywhere outside the blue circle.

northern polar cusp and two in the southern polar cusp. Nevertheless, while the number of nulls in each cluster varies in time (with nulls being created and destroyed in pairs), the locations of the clusters remain relatively steady. Further, if one computes the topological degree of each cluster, one finds that the large-scale topology is consistent with a simple two-null separator topology. This is illustrated in Figure 16, which shows the number of type A nulls (red

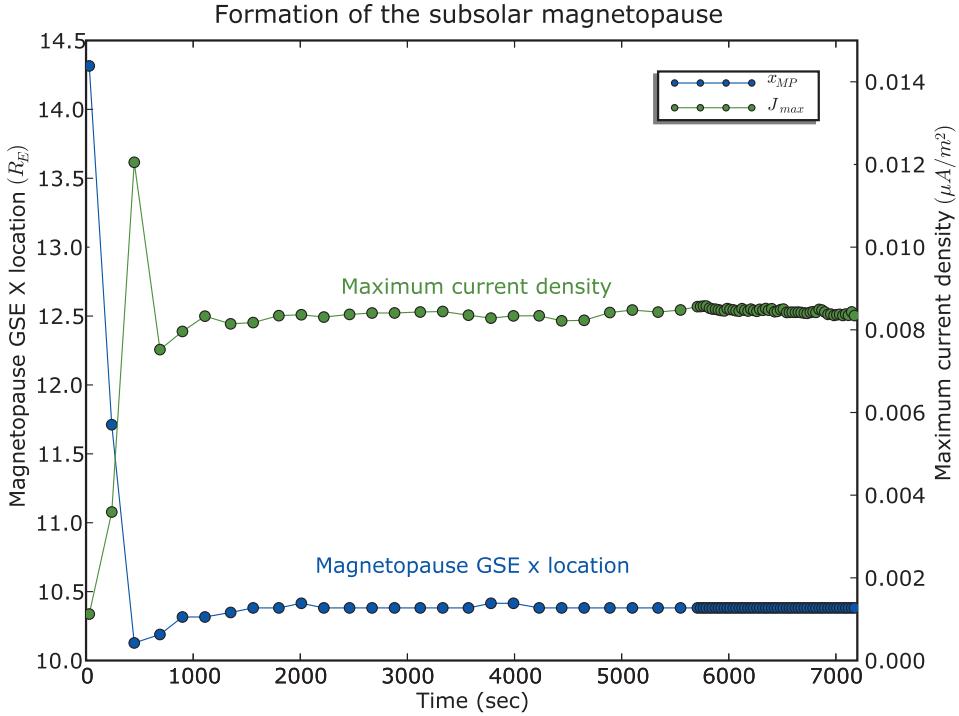

Figure 14. This figure shows the temporal behavior of the maximum current density magnitude in the interval 8.8 $R_E < x < 20$ R_E along the Sun-Earth line in GSE coordinates. We identify this current density maximum as the subsolar magnetopause. A steady state is reached very early in the simulation, after about 1000 s of simulated time.

squares) and type B nulls (blue circles) within each cluster as a function of time. After a steady state has been reached (i.e., after about 1000 s of simulated time), the number of type A nulls in the northernmost cluster always exceeds the number of type B nulls by one; thus this cluster has a topological degree of 1. In contrast, the southernmost cluster has a topological degree of −1. The two intermediate clusters always have equal numbers of type A and type B nulls, corresponding to a vanishing topological degree. This is not surprising, given that nulls must always be created in A-B pairs. Thus the dayside magnetopause magnetic field topology is consistent, on the large scale, with a simple separator topology, despite the fact that the polar cusp topology is more complex (with multiple nulls in each polar cusp). We note that with four clusters of magnetic nulls, the topology shown in Figure 15 bears some resemblance to the "split separator" topology proposed by *Crooker* [1979], in which there are four magnetic nulls on the dayside magnetopause. This resemblance is superficial, however, since two of the null clusters in Figure 15 have vanishing topological degree, whereas all four nulls in the split separator topology have nonvanishing degree.

[44] We argue that magnetopause X lines should be identified with the intersections of the Σ surfaces associated with the cusp magnetic nulls. While there may be small-scale X lines and associated separators joining nulls within a local cluster (we have not yet addressed this interesting question), there is also clearly a large-scale dayside X line which joins nulls in opposite polar cusps. Since this X line extends across the dayside magnetopause from the southern

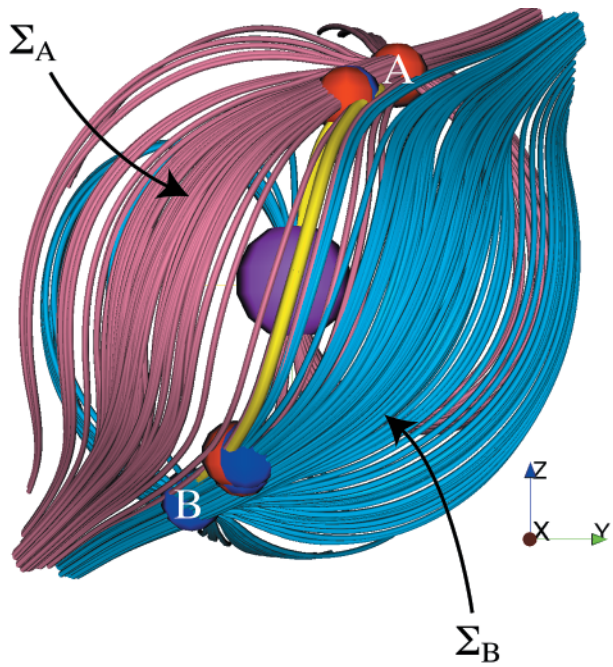

Figure 15. This figure shows the magnetic skeleton computed from the OpenGGCM simulation after 6840 s of simulated time. Type A nulls are shown as red spheres, and type B nulls are the blue spheres. The red lines are magnetic field lines which lie approximately on the Σ_A surface; the blue lines lie approximately on the Σ_B surface. The yellow line is a closed field line which lies approximately at the intersection of the two separatrix surfaces.

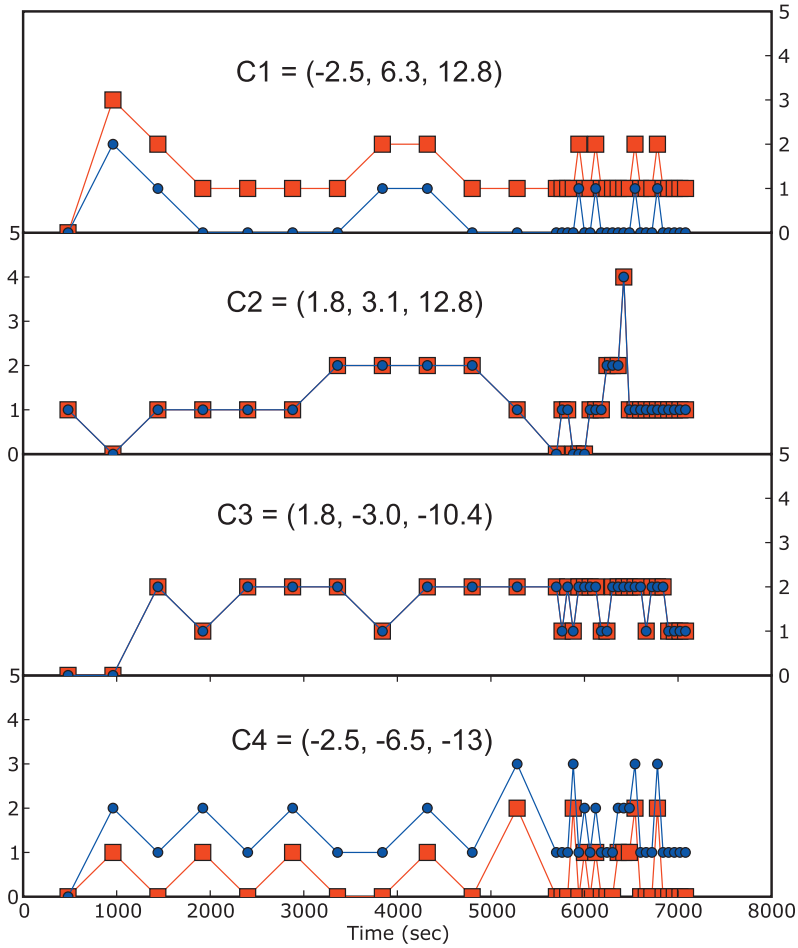

Figure 16. This figure shows the temporal variation of the dayside magnetopause magnetic field topology. The four panels show the number of magnetic nulls within spheres of radius 2 R_E centered at $C1$, $C2$, $C3$, and $C4$, respectively. Red squares show the number of type A nulls, while blue circles show the number of type B nulls.

type B null cluster to the northern type A cluster, the dayside separator line displays properties of both antiparallel reconnection and component reconnection. If one projects the magnetic field line into a plane perpendicular to the large-scale separator line at the subsolar point, on obtains an X type neutral point with a strong guide field. In contrast, if one performs a similar projection at high latitude, one obtains an X type neutral point with a weak guide field. Thus by observing the magnetic field topology at different locations along the separator line, one can obtain results which are consistent with either component reconnection or antiparallel reconnection. The two hypotheses, which at first glance seem to be mutually exclusive, can be viewed as different aspects of a single dayside X line.

2.4. Three-Dimensional Separatrices

[45] The separator topology shown in Figure 15 is consistent with that obtained in previous MHD simulations [*Fedder et al.*, 1995; *Tanaka*, 1999; *Crooker et al.*, 1998; *Siscoe et al.*, 2001; *Watanabe et al.*, 2004]. Nevertheless, as we have previously noted, despite obtaining similar magnetic field topologies, previous studies have differed in their conclusions about the implications of the separator topology for dayside magnetopause reconnection. For example, while *Tanaka* [1999] and *Watanabe et al.* [2004] describe reconnection as a local process associated with magnetic nulls (they make heavy use of two-dimensional magnetic field projections to illustrate such local reconnection processes), *Crooker et al.* [1998] and *Siscoe et al.* [2001] view reconnection as a global process associated with a broad diffusion region on the dayside magnetopause surface. One cannot, on the basis of the magnetic skeleton alone, distinguish between the two interpretations; i.e., one cannot determine the "location" of reconnection from Figure 15, since the magnetic skeleton contains no information about how the parallel electric field is distributed along the separator line.

[46] Figure 17 illustrates the geometry of separator reconnection at the simulated magnetopause. The surface is constructed by computing the set of magnetic field streamlines corresponding to seed points at the nodes of a spherical polar grid ($5\ R_E < r < 15\ R_E$, $0° < \theta < 180°$, $-120° < \phi < 120°$) with dimensions $1000 \times 100 \times 100$. The radial coordinate of the surface, for a given θ and phi, is the location of the last open field line. The surface is painted with the parallel current density, which is proportional to the

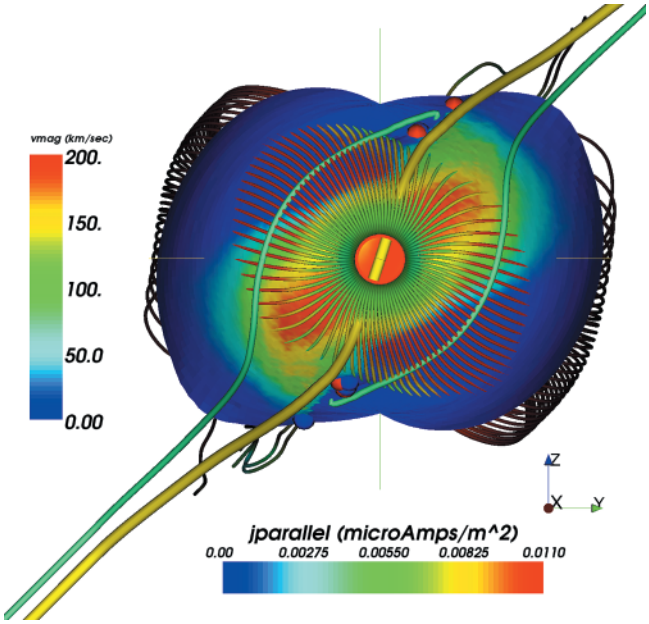

Figure 17. This figure illustrates the geometry of separator reconnection at the OpenGGCM simulated dayside magnetopause. The surface is the boundary between open and solar wind field lines; it is color coded according to the parallel current density. The yellow tube is a solar wind field line just sunward of the subsolar magnetopause; the two green tubes are open field lines which lie on the computed separatrix surface on either side of the separator. Spheres embedded in the surface are type A (red) and type B (blue) nulls. The multicolored tubes are bulk velocity streamlines originating in the solar wind and fanning out around the magnetopause (eventually intersecting the separatrix surface).

parallel electric field, since the Lundquist number has been chosen to be larger than that associated with our discretization errors (e.g., the resistive current sheet is well resolved along this surface). The thick yellow line is a solar wind field line just sunward of the subsolar magnetopause; note how this field line becomes distorted as it approaches the magnetopause: the IMF clock angle is 45 degrees, but the clock angle decreases through the magnetosheath to about 21 degrees just upstream of the magnetopause current sheet. This rotation of the solar wind field line as it approaches the magnetopause is required by the separator topology; the solar wind field line merges into the dayside separator line as it makes contact with the polar cusp nulls in opposite hemispheres.

[47] The colored tubes in Figure 17 are bulk velocity streamlines, computed from seed points distributed in a circle around the Sun-Earth line at GSE z = 15 (in the solar wind). Note that since the surface corresponds to the last open field line, it is only an approximate representation of the actual magnetic separatrix, accurate to about 0.02 R_E (the resolution of the radial search). This is why the two open field lines are visible in the figure, despite the fact that nearby velocity streamlines have not yet crossed the surface. Nevertheless, it is clear that solar wind fluid elements are flowing across the surface separating solar wind field lines from open field lines (note that the flow is steady, so streamlines are the same as fluid element paths); thus according to the *Vasyliunas* [1975] definition of magnetic reconnection, Figure 17 illustrates that separator reconnection can be viewed as a subsolar "component reconnection" process in which solar wind field lines reconnect with closed lines at the separator, producing new open field lines (shown in green).

[48] Interestingly, however, separator reconnection also involves the creation of new closed field lines, as illustrated in Figure 18. This figure is identical to Figure 17, with the exception of the surface, which has been replaced by the boundary between open and closed field lines. Note that the plasma flow around the flanks does not penetrate the surface. Further, the direction of the flow is organized by the the separator line, not the IMF, e.g., the outflow has a "butterfly" pattern with a symmetry axis aligned approximately along the separator line. It is natural to identify this flow as a reconnection outflow emanating from the separator line and confined to the open field line region between the two separatrices. Note, however, that some solar wind plasma has access to closed field lines (i.e., it flows across the surface) in the polar cusps. Thus the separator reconnection process illustrated in Figures 17 and 18 can be divided into two distinct processes: (1) the creation of new overdraped open field lines at low latitudes along the separator; (2) the creation of new closed field lines at high latitudes, near the cusp nulls. The first process can be viewed as a component reconnection

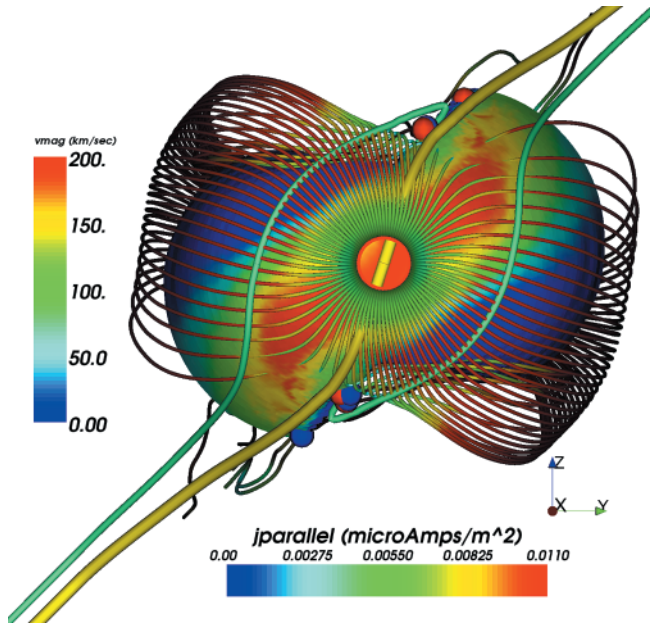

Figure 18. This figure illustrates how dayside magnetopause separator reconnection allows solar wind plasma to flow onto closed field lines. The figure is identical to Figure 17, with the exception of the surface, which is now the boundary between closed and open magnetic field lines. Note that plasma is now flowing across this surface at high latitudes, near the cusp nulls.

process (e.g., in a plane perpendicular to the separator line at low latitude) in which the guide field is large. The second process can be viewed as an example of "double cusp" reconnection in which a solar wind field line makes simultaneous contact with the two polar cusps, producing new closed field lines (as described, for example, by *Song and Russell* [1992]). Rather than being mutually exclusive, both processes, component reconnection and antiparallel reconnection, are different aspects of the same separator reconnection process.

2.5. Three-Dimensional Sweet-Parker Reconnection

[49] The results of the previous two sections demonstrate the following: (1) under generic northward IMF conditions, and when the plasma resistivity is constant, there is a dayside magnetopause X line, a magnetic separator, which extends across the subsolar point, terminating at magnetic nulls in opposite polar cusps; (2) the dayside magnetopause current density takes the form of a broad, thin ribbon which also extends across the subsolar region, terminating in the cusps. However, the geometry of the X line differs from that of the current ribbon: the clock angle of the ribbon (approximately equal to that of the IMF) is larger than the clock angle of the separator ($\approx 21^\circ$). There are good theoretical reasons to expect current sheets to be aligned with separators, in both two [*Dungey*, 1953; *Imshennik and Syrovatsky*, 1967] and three [*Longcope and Cowley*, 1996] dimensions. However, *Longcope and Cowley* [1996] considered the case (appropriate for the solar corona) where the plasma beta is small and the magnetic field evolution is approximately force-free (at least until current sheets form and Alfvénic reconnection outflows impact the dynamics). The plasma beta in the simulated magnetosheath is large, and the plasma flows are significant; thus one cannot appeal to the force-free calculations of *Longcope and Cowley* [1996] to motivate a separator current ribbon at the dayside magnetopause. In other words, while it seems clear that the global separator topology will constrain the dynamics of thin current sheet formation at the dayside magnetopause, it is not obvious that the current sheet should, in the strongly driven high beta magnetosheath/magnetopause system, be aligned with the separator line.

[50] Figure 19 shows the intersections of the two separatrices with the $X_{GSE}-Y_{GSE}$ plane for six different values of Z_{GSE}. The black lines show the separatrix intersections, which themselves intersect to define the intersection of the magnetic separator with the plane. The green arrows illustrate the projection of the bulk velocity field into the plane. The plane is color coded according to the parallel current density. For increasing Z_{GSE}, the Y_{GSE} coordinate of the intersection of the separatrix lines increases. The two separatrix lines (again, these are the intersections of the two separatrix surfaces shown in Figures 17 and 18) seem to merge over a finite region. While the finite length of the merging region is likely an artifact of our inability to numerically resolve the two surfaces (due to errors involved in computing the surfaces), it is clear that the two separatrix lines form an approximate "double Y" geometry which is reminiscent of the two-dimensional Sweet-Parker double Y separatrix geometry. Further, although the local maximum of the parallel current density does not coincide with the magnetic separator (as Figures 17 and 18 demonstrate), the edges of the sheet correspond roughly to the points at which the two separatrix lines diverge.

[51] As newly reconnected open field lines in Figure 18 overdrape (in opposite senses on the positive and negative Y_{GSE} sides of the subsolar point) the magnetopause, they are strongly kinked near the cusp magnetic nulls. In the usual local picture of cusp reconnection, this kinking of the field lines, and the associated plasma flow reversals [see, e.g., *Gosling et al.*, 1990], are identified as signatures of a local reconnection process occurring poleward of the cusp, a solar wind field line is typically visualized as reconnecting with a lobe field line, producing a new overdraped field line. However, Figure 18 clearly shows that the diffusion region (as determined by the parallel current density) extends across the entire dayside magnetopause, rather than being localized at the cusp nulls. Given that global separator reconnection produces new open field lines which are strongly kinked in the cusps (due to the null–null topology), and given that such field line kinking is usually (and unjustifiably, based on field topology alone) identified with a local cusp reconnection process, a natural question arises: Can global separator reconnection produce flow reversals which are traditionally associated with local cusp magnetic reconnection under northward IMF conditions?

[52] Figure 20 is an example of a simulated high-latitude ($Z_{GSE} = 8\ R_E$) flow reversal, in which the Y_{GSE} component of the bulk velocity has a sign opposite to that of the magnetosheath stagnation point outflow for positive Y_{GSE} and Z_{GSE}. This is demonstrated by the fact that the flow reversal, where the Y_{GSE} component of the bulk velocity changes sign, occurs at about (5.6 R_E, 4 R_E), which is also approximately where the two purple separatrix lines intersect. Note also that there is an enhancement of the positive Y_{GSE} component of the bulk flow duskward of the separatrix intersection, in the region between the two separatrices. Note that the intersection of the two purple curves in Figure 20 corresponds to the intersection of the magnetic separator (the X line) with the plane. Thus this simulated flow reversal should be interpreted as a local signature of the global dayside separator reconnection process which occurs at every point along the separator line, including the subsolar point, where the parallel electric field is nonvanishing.

3. Conclusions and Discussion

[53] We have obtained numerical solutions of the three-dimensional resistive magnetohydrodynamics (MHD) equations describing steady magnetic reconnection at Earth's dayside magnetopause under generic northward IMF conditions. The calculation was performed with the OpenGGCM (Open Geospace Global Circulation Model) code, making use of the Zaphod Beowulf cluster www.zaphod.sr.unh.edu) at the University of New Hampshire. This study focused on a single case in which the dipole tilt was zero and the IMF (interplanetary magnetic field) clock angle was 45°. The plasma resistivity was constant in space and time (save for the region within a sphere of radius 6 R_E centered at the origin in GSE coordinates), corresponding to a Lundquist number of 5000 (based on a 1 R_E length scale, the Earth's dipole magnetic field at 1 R_E,

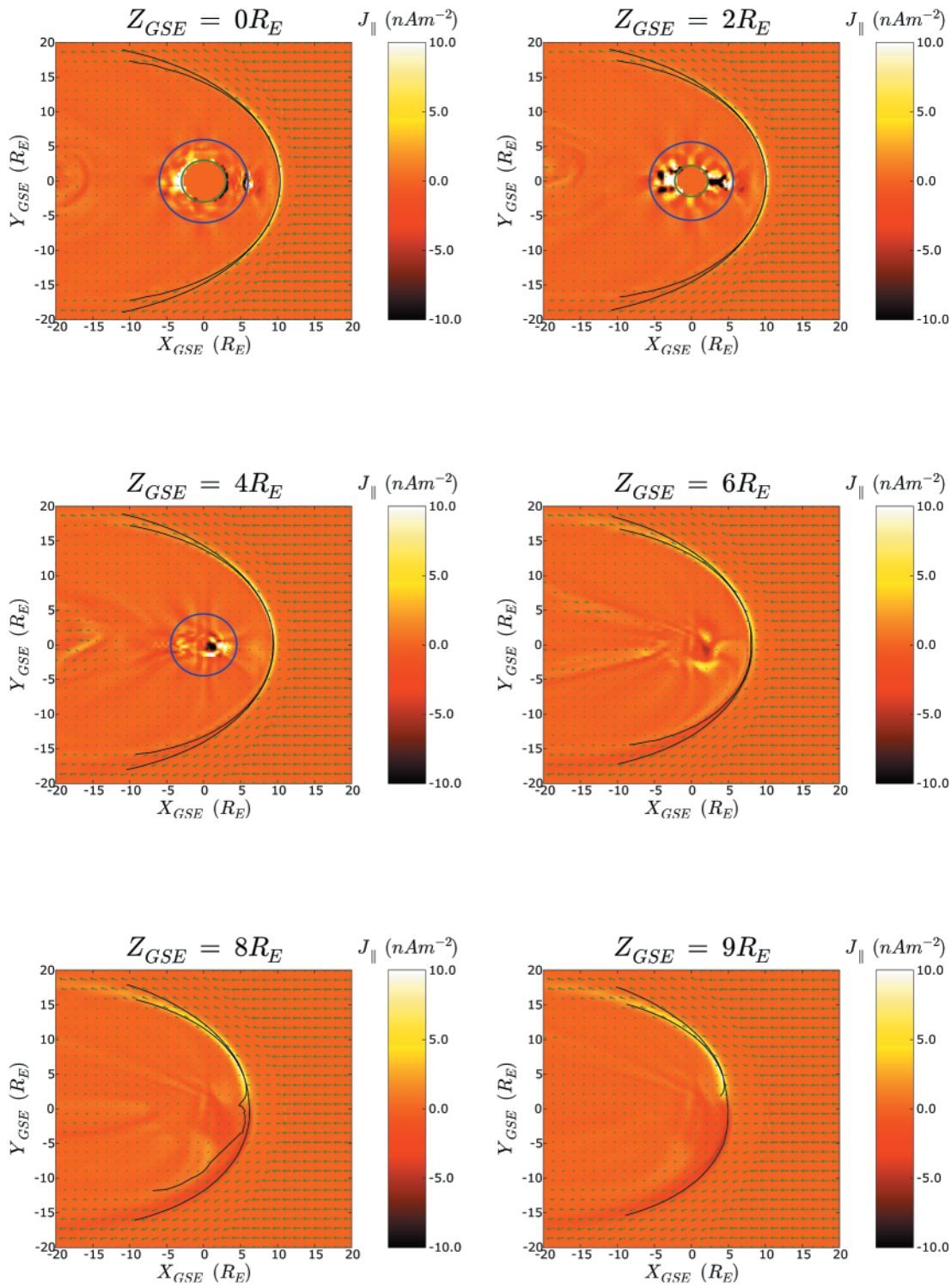

Figure 19. This figure illustrates the double Y geometry of the magnetic separatrices. The black lines show the intersections of the separatrices of Figures 17 and 18 with the $X_{GSE}-Y_{GSE}$ plane at six Z_{GSE} locations. The green arrows show the projected bulk velocity field. The plasma resistivity is zero inside the blue circle. The green circle is the intersection of the inner MHD simulation boundary (where field aligned currents are mapped to the ionosphere).

and a density of 10,000 cm^{-3}). This translates into a Lundquist number of about 1000 based on the average magnetosheath density, magnetic field magnitude, and length scale.

[54] We addressed the following questions in our study: (1) What is the topology of the dayside magnetopause magnetic field under generic northward IMF conditions? (2) What is the geometry of magnetic reconnection at

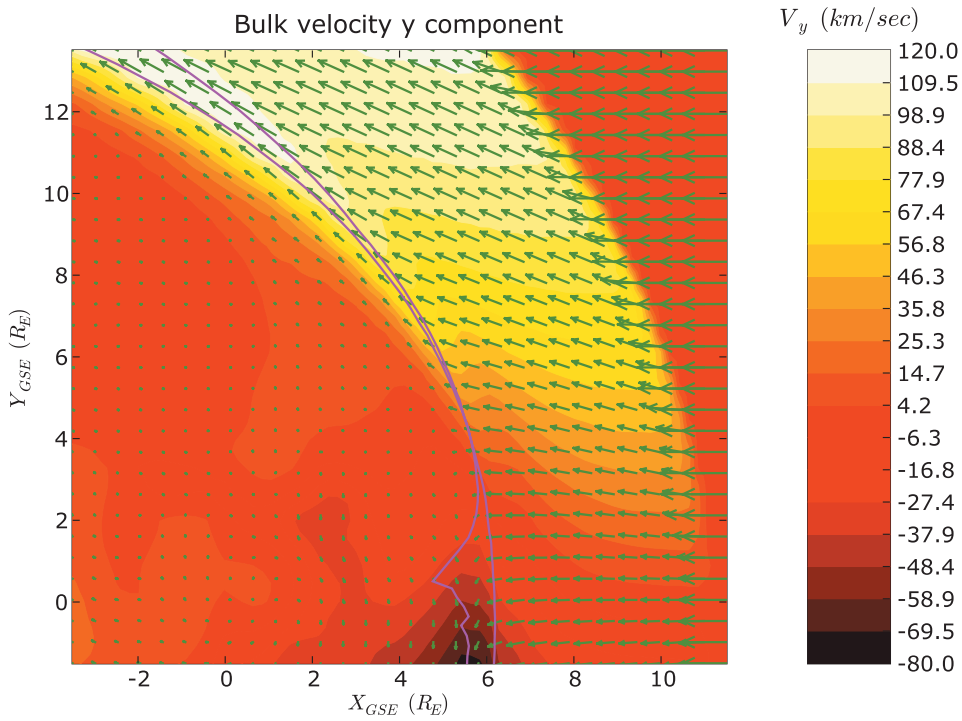

Figure 20. This figure illustrates a simulated high-latitude (Z_{GSE}) reversal of the Y_{GSE} component of the plasma bulk velocity associated with separator reconnection. The purple lines show the intersections of the magnetic separatrices with the plane. The green arrows show the projected bulk velocity vectors.

Earth's dayside magnetopause under generic northward IMF conditions? (i.e., how is current density distributed on the magnetopause surface?).

[55] Our results can be summarized as follows:

[56] 1. The dayside magnetopause magnetic field topology is characterized by two clusters of magnetic nulls, one in the northern polar cusp and one in the southern polar cusp. While the number of nulls in the two clusters varies in time, the locations of the clusters are very steady, as is the location of the magnetopause current sheet.

[57] 2. While the magnetic topology in the cusps is complex, consisting of multiple type A and type B nulls being created and annihilated in pairs, the large-scale topology is simple, i.e., the topological degree of the northern cluster is 1, while the topological degree of the southern cluster is -1. Further, the magnetic skeleton is consistent, on the large scale, with a null–null separator topology, with the dayside X line extending across the subsolar magnetopause and terminating in the cusps.

[58] 3. Current density is distributed in a broad, thin ribbon which extends across the dayside magnetopause and terminates in the polar cusps. While the axis of the ribbon does not coincide with the separator, the edges of the ribbon correspond closely to the locations where the two three-dimensional separatrix surfaces diverge.

[59] 4. The geometry of dayside separator reconnection displays features of both component and antiparallel reconnection. Near the subsolar point, plasma flows around the flanks of the magnetopause perpendicular to the separator line, crossing the boundary between solar wind field lines and open field lines (thus producing new overdraped open field lines); in the cusps, solar wind plasma flows onto closed field lines as solar wind field lines approach the separator (the intersection of the two separatrix surfaces). While new open field lines are strongly kinked in the cusps, this is due to the null–null separator topology and not due to a local reconnection process in the cusps, the parallel electric field is not localized to the cusps.

[60] An important implication of conclusions 1–4 above is that one cannot identify magnetic reconnection with local properties of the magnetic field topology. In particular, one cannot, by identifying cusp magnetic nulls and associated kinked magnetic field lines, infer that reconnection is a local process which occurs at a null. While it is certainly possible for local current sheets to form near isolated magnetic nulls, reconnection at such nulls is qualitatively different from that associated with two-dimensional nulls or three-dimensional null–null lines (e.g., there is only one magnetic separatrix associated with an isolated three-dimensional null). Without determining the global topology of the magnetic field, by constructing a global picture of the magnetic interconnections (via separator lines) among nulls, one cannot obtain a complete picture of the reconnection topology. For example, it is clear that our simulated magnetopause has X lines which join nulls in opposite cusps.

[61] Another interesting feature of the reconnection observed at our simulated magnetopause is the global nature of the diffusion region. The diffusion region is not localized in the cusps (contrary to the traditional "double cusp" northward IMF reconnection cartoon [*Dungey*, 1963; *Song*

and Russell, 1992]). Instead, the diffusion region appears to be closely associated with the region of space where the two three-dimensional magnetic separatrices make contact. While the geometry of the separatrix intersection is reminiscent of the typical Sweet-Parker double Y topology, we have not yet been able to determine whether the separatrices make contact over a finite region, i.e., whether the separator is a ribbon or a line is an interesting unresolved issue.

[62] We end with some further caveats and suggestions for future work. We have not addressed the issue of the plasma resistivity model. Ideal MHD cannot model the kinetic processes in the diffusion region which give rise to violations of the frozen flux theorem; therefore we must explicitly add nonideal terms to Ohm's law in order to produce magnetic reconnection which is not a result of numerical diffusion. For the sake of simplicity, and in order to make contact with previous numerical and analytic work, we have used constant plasma resistivity in our simulation, making sure that our explicit resistivity is larger than the numerical resistivity. Since it is well known that the plasma resistivity model can have a significant impact on the geometry of two-dimensional reconnection diffusion regions (e.g., the *Petschek* [1964] slow shock model can be recovered in resistive MHD simulations when the plasma resistivity is localized in such a way that the length and width of the diffusion region are proportional to the resistivity), an interesting extension of the present work would be a study of the effects of the plasma resistivity model on the topology and geometry of dayside magnetopause reconnection. Further, while it is interesting and encouraging that we have obtained simulation results which are reminiscent of two-dimensional Sweet-Parker reconnection, our results also suggest that resistive MHD is incapable of modeling fast reconnection in the high Lundquist number limit (owing to the well known Sweet-Parker timescale problem).

[63] Finally, we have not yet made an attempt to predict observable spacecraft signatures of separator reconnection. While Figure 20 suggests that local plasma flow signatures which have traditionally been identified with local cusp reconnection might also be consistent with separator reconnection, we have not yet performed any detailed analyses to compare our simulation with observations. Some of the questions which might be addressed include: Can the kinked magnetic field lines near the nulls at the ends of the separator be approximated as one-dimensional rotational discontinuities (as one assumes, for example, when performing the Walén tangential stress balance test [*Hudson*, 1970; *Sonnerup*, 1981] at the magnetopause)? Can separator reconnection produce plasma flow reversals which are consistent with those observed by spacecraft? What are the observable signatures of separator reconnection at the low shear subsolar magnetopause? Are observed cusp ion dispersion signatures and ion D-shaped distributions consistent with a global separator topology? While some of these questions (ion dispersion and D-shaped distributions) are beyond the scope of resistive MHD, it may be possible to address them in a qualitative way with test particle simulations.

[64] **Acknowledgments.** This research was made possible by the following grants: NASA NNG05GE87G and NNG05G158G; NSF ATM-0503268, ATM-0543202, ATM-0422764, ATM-0420905, and ATM-0503189; and DOE DE-FG02-05ER54832. Global MHD computations were carried out on the Zaphod Beowulf cluster at the UNH Institute for the Study of Earth, Oceans and Space.

[65] Wolfgang Baumjohann thanks John Finn and another reviewer for their assistance in evaluating this paper.*

References

Axford, W. I. (1984), Magnetic reconnection, in *Magnetic Reconnection in Space and Astrophysical Plasmas*, *Geophys. Monogr. Ser.*, vol. 30, edited by J. E. W. Hones, p. 1, AGU, Washington, D. C.

Boozer, A. H. (2002), Reconnection and the ideal evolution of magnetic fields, *Phys. Rev. Lett.*, *88*, 215,005.

Chandler, M. O., S. A. Fuselier, M. Lockwood, and T. E. Moore (1999), Evidence of component merging equatorward of the cusp, *J. Geophys. Res.*, *104*, 22,623–22,633.

Coleman, I. J., G. Chisham, M. Pinnock, and M. P. Freeman (2001), An ionospheric convection signature of antiparallel reconnection, *J. Geophys. Res.*, *106*, 28,995–29,007.

Cowley, S. W. H. (1973), A qualitative study of the reconnection between the earth's magnetic field and an interplanetary field of arbitrary orientation, *Radio Sci.*, *8*, 903–913.

Cowley, S. W. H. (1976), Comments on the merging of nonantiparallel magnetic fields, *J. Geophys. Res.*, *81*, 3455–3458.

Cowley, S. W. H. (1982), The causes of convection in the earth's magnetosphere: A review of developments during the ims, *Rev. Geophys.*, *20*, 531–565.

Cowley, S. W. H. (1983) Interpretation of observed relationsh between solar wind characteristics and effects at ionospheric altitudes, in *High Latitude Space Plasma Physics*, edited by B. Hultqvist and T. Hagfors, pp. 225–249, Springer, New York.

Crooker, N. (1979), Dayside merging and cusp geometry, *J. Geophys. Res.*, *84*, 951–959.

Crooker, N. U. (1992), Reverse convection, *J. Geophys. Res.*, *97*, 19,363–19,372.

Crooker, N. U., J. G. Lyon, and J. A. Fedder (1998), Mhd model merging with imf b_y: Lobe cells, sunward polar cap convection, and overdraped lobes, *J. Geophys. Res.*, *103*, 9143–9151.

Daughton, W., G. Lapenta, and P. Ricci (2004), Nonlinear evolution of the lower-hybrid drift instability in a current sheet, *Phys. Rev. Lett.*, *93*, 105,004.

Dorelli, J. C., M. Hesse, M. Kuznetsova, L. Rastaetter, and J. Raeder (2004), A new look at driven magnetic reconnection at the terrestrial dayside magnetopause, *J. Geophys. Res.*, *109*, A12216, doi:10.1029/2004JA010458.

Dungey, J. W. (1953), Conditions for the occurrence of electrical discharges in astrophysical systems, *Phil. Mag.*, *44*, 725–738.

Dungey, J. W. (1961), Interplanetary magnetic field and the auroral zones, *Phys. Rev. Lett.*, *6*, 47–48.

Dungey, J. W. (1963) The structure of the exosphere, or adventures in velocity space, in *Geophysics, The Earth's Environment*, edited by C. DeWitt, J. Hieblot, and A. Lebeau, p. 505, Gordon and Breach, New York.

Evans, C. R., and J. F. Hawley (1988), Simulation of magnetohydrodynamic flows: A constrained transport method, *Astrophy. J.*, *332*, 659–677.

Fedder, J. A., J. G. Lyon, S. P. Slinker, and C. M. Mobarry (1995), Topological structure of the magnetotail as a function of interplanetary magnetic field direction, *J. Geophys. Res.*, *100*, 3613–3621.

Fuselier, S. A., B. J. Anderson, and T. G. Onsager (1997), Electron and ion signatures of field line topology at the low-shear magnetopause, *J. Geophys. Res.*, *102*, 4847–4863.

Fuselier, S. A., K. J. Trattner, and S. M. Petrinec (2000), Cusp observations of high- and low-latitude reconnection for northward interplanetary magnetic field, *J. Geophys. Res.*, *105*, 255–266.

Fuselier, S. A., H. U. Frey, K. J. Trattner, S. B. Mende, and J. L. Burch (2002), Cusp aurora dependence on interplanetary magnetic field b_z, *J. Geophys. Res.*, *107*(A7), 1111, doi:10.1029/2001JA900165.

Gosling, J. T., J. R. Asbridge, S. J. Bame, W. C. Feldman, G. Paschmann, and N. Sckopke (1982), Evidence for quasi-stationary reconnection at the dayside magnetopause, *J. Geophys. Res.*, *87*, 2147–2158.

Gosling, J. T., M. F. Thomsen, S. J. Bame, R. C. Elphic, and C. T. Russell (1990), Plasma flow reversals at the dayside magnetopause and the origin of asymmetric polar cap convection, *J. Geophys. Res.*, *95*, 8073–8084.

Gosling, J. T., M. F. Thomsen, S. J. Bame, and R. C. Elphic (1991), Observations of reconnection of interplanetary and lobe magnetic field lines at the high latitude magnetopause, *J. Geophys. Res.*, *96*, 14,097–14,106.

Greene, J. (1988), Geometric properties of three-dimensional reconnecting fields with magnetic nulls, *J. Geophys. Res.*, *93*, 8583–8590.

Greene, J. (1992), Locating three-dimensional roots by a bisection method, *J. Comput. Phys.*, *98*, 194–198.

*The acknowledgments are ccorrect here. The article as originally published is online.

Hesse, M., and K. Schindler (1988), A theoretical foundation of general magnetic reconnection, *J. Geophys. Res.*, *93*, 5559–5567.

Hu, S., A. Bhattacharjee, J. Dorelli, and J. M. Greene (2004), The spherical tearing mode, *Geophys. Res. Lett.*, *31*, L19806, doi:10.1029/2004GL020977.

Hudson, P. D. (1970), Discontinuities in an anisotropic plasma and their identification in the solar wind, *Planet. Space Sci.*, *18*, 1611–1622.

Imshennik, V. S., and S. I. Syrovatsky (1967), Two-dimensional flow of an ideally conducting gas in the vicinity of the zero line of a magnetic field, *Sov. Phys. JETP*, *25*, 656–664.

Karimabadi, H. (2005), Antiparallel versus component merging at the magnetopause: Current bifurcation and intermittent reconnection, *J. Geophys. Res.*, *110*, A03213, doi:10.1029/2004JA010750.

Kessel, R. L., S.-H. Chen, J. L. Green, S. F. Fung, S. A. Boardsen, L. C. Tan, T. E. Eastman, J. D. Craven, and L. A. Frank (1996), Evidence for high-latitude reconnection during northward imf: Hawkeye observations, *Geophys. Res. Lett.*, *23*, 583–586.

Kronecker, L. (1869), Ueber systeme von funktionen mehrerer variabeln, *Monatsber. Berlin Akad.*, 159–193, 688–698.

Lau, Y.-T., and J. Finn (1990), Three-dimensional kinematic reconnection in the presence of field nulls and closed field lines, *Astrophys. J.*, *350*, 672–691.

Lavraud, B., et al. (2002), Cluster observations of the exterior cusp and its surrounding boundaries under northward imf, *Geophys. Res. Lett.*, *29*(20), 1995, doi:10.1029/2002GL015464.

Le, G., J. Raeder, C. T. Russell, G. Lu, M. Petrinec, and F. S. Mozer (2001), Polar cusp and vicinity under strongly northward interplanetary magnetic field on April 11, 1997: Observations and mhd, *J. Geophys. Res.*, *106*, 21,083–21,093.

Li, W., J. Raeder, J. Dorelli, M. Oieroset, and T. D. Phan (2005), Plasma sheet formation during long period of northward imf, *Geophys. Res. Lett.*, *32*, L12S08, doi:10.1029/2004GL021524.

Li, X. (1999), A 16 moment fast solar wind model, *Space Sci. Rev.*, *87*, 253–256.

Longcope, D. W., and S. C. Cowley (1996), Current sheet formation along three-dimensional magnetic separators, *Phys. Plasmas*, *3*, 2885–2897.

Newcomb, W. A. (1958), Motion of magnetic lines of force, *Ann. Phys.*, *3*, 347–385.

Onsager, T. E., J. D. Scudder, M. Lockwood, and C. T. Russell (2001), Reconnection at the high-latitude magnetopause during northward interplanetary magnetic field conditions, *J. Geophys. Res.*, *106*, 25,467–25,488.

Parker, E. N. (1957), Sweet's mechanism for merging magnetic fields in conducting fluids, *J. Geophys. Res.*, *62*, 509.

Paschmann, G., W. Baumjohann, N. Sckopke, T.-D. Phan, and H. Lühr (1993), Structure of the dayside magnetopause for low magnetic shear, *J. Geophys. Res.*, *98*, 13,409.

Petrinec, S. M., and S. A. Fuselier (2003), Comment on "An ionospheric convection signature of antiparallel reconnection" by Coleman et al., *J. Geophys. Res.*, *108*(A5), 1177, doi:10.1029/2002JA009421.

Petschek, H. E. (1964), Magnetic field annihilation, in AAS-NASA Symposium on Physics of Solar Flares, *NASA Spec. Publ.*, *50*, 425–439.

Phan, T., et al. (2003), Simultaneous cluster and image observations of cusp reconnection and auroral proton spot northward imf, *Geophys. Res. Lett.*, *30*(10), 1509, doi:10.1029/2003GL016885.

Polymilis, C., G. Servizi, C. Skokos, G. Turchetti, and M. N. Vrahatis (2003), Topological degree theory and local analysis of area preserving maps, *Chaos*, *13*, 94–104.

Priest, E. R., and T. G. Forbes (2000) *Magnetic Reconnection: MHD Theory and Applications*, chap. 4, pp. 123–125, Cambridge Univ. Press, New York.

Quest, K. B., and F. V. Coroniti (1981), Tearing at the dayside magnetopause, *J. Geophys. Res.*, *86*, 3289–3298.

Raeder, J. (1999), Modeling the magnetosphere for northward interplanetary magnetic field: Effects of electrical resistivity, *J. Geophys. Res.*, *104*, 17,357–17,367.

Raeder, J. (2003), Global geospace modeling: Tutorial and review, in *Space Plasma Simulation*, edited by J. B. Büchner, C. T. Dum, and M. Sholer, Springer, New York.

Raeder, J., R. J. Walker, and M. Ashour-Abdalla (1995), The structure of the distant geomagnetic tail during long periods of northward imf, *Geophys. Res. Lett.*, *22*, 349–352.

Raeder, J., et al. (2001), Global simulation of the geospace environment modeling substorm challenge event, *J. Geophys. Res.*, *106*, 381.

Rogers, B. N., R. E. Denton, J. F. Drake, and M. A. Shay (2001), The role of dispersive waves in collisionless magnetic reconnection, *Phys. Rev. Lett.*, *87*, 195,004.

Russell, C. (1972), The configuration of the magnetosphere, in *Critical Problems of Magnetospheric Physics*, edited by E. R. Dryer, pp. 1–16, IUCSTP Secretariat, Washington, D. C.

Russell, C. T., and G. Le (2000), Cusp observations of high- and low-latitude reconnection: An alternate view, *J. Geophys. Res.*, *105*, 5489–5495.

Russell, C. T., et al. (1998), Entry of the polar spacecraft into the polar cusp under northward imf conditions, *Geophys. Res. Lett.*, *25*, 3015–3018.

Schindler, K., and M. Hesse (1988), General magnetic reconnection, parallel electric fields, and helicity, *J. Geophys. Res.*, *93*, 5547–5557.

Scudder, J. D., F. S. Mozer, N. C. Maynard, and C. T. Russell (2002), Fingerprints of collisionless reconnection at the separator i: Ambipolar-hall signatures, *J. Geophys. Res.*, *107*(A10), 1294, doi:10.1029/2001JA000126.

Siscoe, G. L., G. M. Erickson, B. U. O. Sonnerup, N. C. Maynard, K. D. Siebert, D. R. Weimer, and W. W. White (2001), Global role of $e_{||}$ in magnetopause reconnection: An explicit demonstration, *J. Geophys. Res.*, *106*, 13,015–13,022.

Song, P., and C. T. Russell (1992), Model of the formation of the low-latitude boundary layer for strongly northward interplanetary magnetic field, *J. Geophys. Res.*, *97*, 1411–1420.

Sonnerup, B. U. O. (1974), The magnetopause reconnection rate, *J. Geophys. Res.*, *79*, 1546–1549.

Sonnerup, B. U. O. (1981), Evidence for magnetic field reconnection at Earth's magnetopause, *J. Geophys. Res.*, *86*, 10,049–10,067.

Sonnerup, B. U. O., and E. R. Priest (1975), Resistive mhd stagnation-point flows at a current sheet, *J. Plasma Phys.*, *14*, 283–294.

Swisdak, M., B. N. Rogers, J. F. Drake, and M. A. Shay (2003), Diamagnetic suppression of component magnetic reconnection at the magnetopause, *J. Geophys. Res.*, *108*(A5), 1218, doi:10.1029/2002JA009726.

Syrovatsky, S. I. (1971), Formation of current sheets in a plasma with frozen-in strong magnetic field, *Sov. Phys. JETP*, *33*, 933.

Tanaka, K. G., I. Shinohara, and M. Fujimoto (2004), Effects of guide field on quick mangetic reconnection triggering, *Geophys. Res. Lett.*, *31*, L22806, doi:10.1029/2004GL021191.

Tanaka, T. (1999), Configuration of the magnetosphere-ionosphere convection system under northward imf conditions with nonzero imf b_y, *J. Geophys. Res.*, *104*, 14,683–14,690.

Trattner, K. J., S. A. Fuselier, and S. M. Fuselier (2004), Location of the reconnection line for northward interplanetary magnetic field, *J. Geophys. Res.*, *109*, A03219, doi:10.1029/2003JA009975.

Tsyganenko, N. A. (1995a), Modeling the earth's magnetospheric magnetic field confined within a realistic magnetopause, *J. Geophys. Res.*, *100*, 5599–5612.

Tsyganenko, N. A. (1995b), Modeling the earth's magnetospheric magnetic field confined within a realistic magnetopause, *J. Geophys. Res.*, *100*, 5599.

Tsyganenko, N. A. (1996) Effects of the solar wind conditions on the global magnetospheric configuration as deduced from data-based field models, in *Proceedings of the ICS-3 Conference on Substorms*, *Eur. Space Agency Spec. Publ.*, *ESA SP-389*, 181.

Tsyganenko, N. A., and D. P. Stern (1996), Modeling the global magnetic field of the large-scale birkeland current systems, *J. Geophys. Res.*, *100*, 27,187–27,198.

Vasyliunas, V. M. (1968), A survey of low-energy electrons in the evening sector of the magnetosphere with ogo 1 and ogo 3, *J. Geophys. Res.*, *73*, 2839–2884.

Vasyliunas, V. M. (1972), Nonuniqueness of magnetic field line motion, *J. Geophys. Res.*, *77*, 6271–6274.

Vasyliunas, V. M. (1975), Theoretical models of magnetic field line merging, *Rev. Geophys.*, *13*, 303.

Watanabe, M., G. J. Sofko, D. A. André, T. Tanaka, and M. R. Hairston (2004), Polar cusp bifurcation during steady-state northward interplanetary magnetic field with $|b_y| \sim |b_z|$, *J. Geophys. Res.*, 109,A01215, doi:10.1029/2003JA009944.

Weibel, E. S. (1959), Spontaneously growing transverse waves in a plasma due to an anisotropic velocity distribution, *Phys. Rev. Lett.*, *2*, 83.

A. Bhattacharjee, J. C. Dorelli, and J. Raeder, EOS Space Science Center, University of New Hampshire, 39 College Road, Durham, NH, 03824, USA. (john.dorelli@unh.edu)